J. Fluid Mech. (2016), *vol.* 791, *pp.* 61–96. © Cambridge University Press 2016
doi:10.1017/jfm.2016.43

Helical mode interactions and spectral transfer processes in magnetohydrodynamic turbulence

Moritz Linkmann[1,†], Arjun Berera[1], Mairi McKay[1] and Julia Jäger[1]

[1]School of Physics and Astronomy, University of Edinburgh, Edinburgh EH9 3FD, UK

(Received 1 September 2015; revised 18 November 2015; accepted 8 January 2016;
first published online 15 February 2016)

Spectral transfer processes in homogeneous magnetohydrodynamic (MHD) turbulence are investigated analytically by decomposition of the velocity and magnetic fields in Fourier space into helical modes. Steady solutions of the dynamical system which governs the evolution of the helical modes are determined, and a stability analysis of these solutions is carried out. The interpretation of the analysis is that unstable solutions lead to energy transfer between the interacting modes while stable solutions do not. From this, a dependence of possible interscale energy and helicity transfers on the helicities of the interacting modes is derived. As expected from the inverse cascade of magnetic helicity in 3-D MHD turbulence, mode interactions with like helicities lead to transfer of energy and magnetic helicity to smaller wavenumbers. However, some interactions of modes with unlike helicities also contribute to an inverse energy transfer. As such, an inverse energy cascade for non-helical magnetic fields is shown to be possible. Furthermore, it is found that high values of the cross-helicity may have an asymmetric effect on forward and reverse transfer of energy, where forward transfer is more quenched in regions of high cross-helicity than reverse transfer. This conforms with recent observations of solar wind turbulence. For specific helical interactions the relation to dynamo action is established. The present analysis provides new theoretical insights into physical processes where inverse cascade and dynamo action are involved, such as the evolution of cosmological and astrophysical magnetic fields and laboratory plasmas.

Key words: homogeneous turbulence, MHD turbulence, turbulence theory

1. Introduction

Since the contributions by Richardson and Kolmogorov it is well established that the average transfer of kinetic energy occurring in isotropic non-conducting turbulent fluids in three dimensions proceeds from the large scales to the small scales, or, in the Fourier representation, from small to large wavenumbers (see e.g. Frisch 1995, McComb 2014). However, many turbulent flows occurring in nature and/or in industrial applications deviate from this behaviour, showing some backwards energy transfer. Examples include rotating flows (Mininni, Alexakis & Pouquet 2009), two-dimensional flows (e.g. Kraichnan 1967; Boffetta & Musacchio 2010; Mininni & Pouquet 2013) and flows doped with polymeric additives (Dubief, Terrapon & Soria 2013).

† Email address for correspondence: m.linkmann@ed.ac.uk

Electrically conducting turbulent flows also show a variety of phenomena resulting in a transfer of energy from the small scales to the large scales (Biskamp 1993). One of these is the inverse cascade of magnetic helicity, first proposed by Frisch *et al.* (1975) after the derivation of absolute equilibrium spectra for magnetic and kinetic energies as well as cross and magnetic helicities, and which was subsequently confirmed numerically (Pouquet, Frisch & Léorat 1976; Pouquet & Patterson 1978). By virtue of the realisability condition, which states that magnetic energy at a given wavenumber k is bounded from below by $k/2$ times the magnitude of the magnetic helicity (see e.g. Moffatt 1978, Biskamp 1993), it also drives a transfer of magnetic energy from the small to the large scales. Another process, which is of particular importance in astrophysical fluid dynamics due to the generation of magnetic fields of astrophysical bodies, is the large-scale dynamo, by which a magnetic field on scales larger than the typical scale of the largest eddies is generated from a magnetic seed field. The α-effect of mean-field electrodynamics is a classic example of a large-scale dynamo, and it relies on the presence of kinetic helicity (Krause & Rädler 1980; Brandenburg 2001). Thus in both these cases energy is transferred in spectral space from large to small wavenumbers, and a lack of mirror symmetry (i.e. the presence of kinetic and/or magnetic helicity) facilitates these types of energy transfer. Moreover, results from recent numerical simulations (Berera & Linkmann 2014; Zrake 2014; Brandenburg, Kahniashvili & Tevzadze 2015) show that some kind of inverse spectral transfer also occurs in conducting flows with vanishing magnetic and kinetic helicities. Recently, Stepanov, Frick & Mizeva (2015) calculated energy and helicity transfer fluxes numerically from a helical shell model, where helicity and energy input were separated in order to test the influence of magnetic helicity on the turbulent dynamics. They found that the inverse cascade of magnetic helicity is connected to a transfer of purely magnetic energy to lower wavenumbers. By alternating the sign of helicity injected into the system it was shown that even if the average injection rate of magnetic helicity vanishes, the reverse transfer of magnetic energy induced by the instantaneous injection of magnetic helicity remains active.

The effect of helicity on energy transfer and evolution in non-conducting turbulent fluids has received considerable attention (Moffatt 1969; André & Lesieur 1977; Pelz, Shtilman & Tsinober 1986; Polifke & Shtilman 1989; Polifke 1991; Waleffe 1992; Chen, Chen & Eyink 2003*a*; Chen *et al.* 2003*b*; Biferale, Musacchio & Toschi 2012, 2013; Biferale & Titi 2013). It has been studied in a variety of ways, e.g. using analytical methods, closure calculations, conventional direct numerical simulations (DNS) and novel approaches in DNS. Waleffe (1992) decomposed the Fourier transform of the velocity field into eigenfunctions of the curl operator and derived evolution equations for these eigenfunctions by substitution of the decomposed field into the Navier–Stokes equation for incompressible flow. Since the non-zero eigenvalues of the corresponding eigenfunctions are related to the helicity of a given velocity field mode, the evolution equations were further analysed in order to derive the dependence of the possible energy transfers on the helicities of the interacting modes. If the largest two wavenumbers of a given wavevector triad had helicities of opposite sign, energy was transferred forward in wavenumber space, while a reverse transfer of energy became possible if the helicities were of the same sign. The analysis also showed that the triads responsible for an inverse energy cascade contribute to a direct cascade of kinetic helicity. The possibility of an inverse cascade of kinetic energy and a forward cascade of kinetic helicity had previously been predicted by Brissaud *et al.* (1973).

Biferale *et al.* (2012) investigated numerically whether this reverse spectral transfer caused by interactions of helical modes of the same sign occurs. By defining a

projection operation on the nonlinear term the authors altered the Navier–Stokes equation to ensure that only modes of, say, positive helicity were present in the system. The altered Navier–Stokes equation was subsequently solved numerically using the standard pseudospectral method in conjunction with small-scale forcing. As predicted by Waleffe's analysis, it was found that kinetic energy was indeed transferred downwards in wavenumber space. This was the first observation of an inverse energy cascade in three-dimensional isotropic turbulence.

In a subsequent paper (Biferale *et al.* 2013), the same authors forced the system at the large scales in order to study the predicted forward cascade of kinetic helicity, which was indeed observed in the simulations. Since the subset of positively helical modes does not transfer energy to the small scales, it was expected that the resulting dynamical system would not show finite dissipation in the limit of infinite Reynolds number. Hence the projected Navier–Stokes equation which governs the evolution should be globally regular, which was subsequently proven by Biferale & Titi (2013).

Thus, in summary, the decomposition of the Fourier transform of the turbulent velocity field fluctuations into helical modes has been proven to be very useful in terms of understanding some fundamental features of turbulent flows, which go beyond the established Kolmogorov–Richardson (direct) cascade of kinetic energy. In view of the effects of kinetic and magnetic helicities on the direction of energy transfer in magnetohydrodynamic (MHD) turbulence, and inspired by the successes of the helical decomposition used in hydrodynamics, in this paper we propose to use the decomposition of both the magnetic and velocity fields into helical modes in order to perhaps shed some more light on why MHD turbulence shows much more transfer from the small scales to the large scales than turbulence in non-conducting fluids. This analysis provides deeper insight into fundamental transfer processes in MHD turbulence. It will help in the further theoretical understanding of various physical processes involving inverse cascade and dynamo action, such as the evolution and generation of cosmological and galactic magnetic fields.

Before outlining the structure of this paper we pause briefly to discuss the terminology used. As the precise meaning of the term varies in the literature, it is not always evident what is meant by an inverse cascade. In the astrophysical literature, transfer of energy and helicity from higher to lower wavenumbers is often described as an inverse cascade (Son 1999; Christensson, Hindmarsh & Brandenburg 2001; Cho 2011), while the fluid dynamics literature requires any cascade process to possess a wavenumber-independent flux (Alexakis, Mininni & Pouquet 2006; Biferale *et al.* 2012; Müller, Malapaka & Busse 2012; Biferale & Titi 2013; McComb 2014; Brandenburg *et al.* 2015). It is thus of interest to not only classify the different types of reverse transfer that can occur in MHD turbulence, but also to perhaps clarify the terminology. Therefore we propose in this paper the general term reverse (or inverse) spectral transfer, which encompasses all the phenomena described above as subcategories according to their properties. We define it as any process that produces an increase in a spectral quantity (total energy, magnetic helicity, etc.) at low wavenumbers due to transfer of that quantity away from higher wavenumbers into smaller wavenumbers. In this framework an inverse cascade is a reverse spectral transfer showing constant flux of the cascading quantity over a certain wavenumber range. We point out that in MHD concerns have been raised over the use of the term 'cascade' (Müller *et al.* 2012), as it may be understood to imply energy (or magnetic helicity) transfer mainly due to local interactions, which might not be the case in MHD turbulence (Alexakis, Mininni & Pouquet 2005; Debliquy, Verma & Carati 2005; Cho 2010; Müller *et al.* 2012). We will come back to this point in the discussion section of this paper.

This paper is organised as follows. First we explain the helical decomposition of the velocity and magnetic fields in § 2 and use this decomposition to outline the derivation of the evolution equations for the helical coefficients from the MHD equations in § 3 following the work by Lessinnes, Plunian & Carati (2009). This leads to a system of coupled ordinary differential equations (ODEs) describing the interaction of modes corresponding to a single triad of wavenumbers. In §§ 4 and 5 the linear stability of steady solutions of this system is examined. Section 6 explains the assumptions used to interpret results from the stability analysis followed by a presentation of first results on energy transfers, which are used in § 7 to calculate the contribution to inertial range energy and magnetic helicity cascades. In § 8 we analyse specific cases where the MHD equations can be decoupled and relate our analysis to large- and small-scale kinematic dynamo results such as the α-effect (Moffatt 1978; Parker 1979; Krause & Rädler 1980). Our results are summarised and discussed in § 9 in the context of numerical simulations of MHD turbulence and observations of turbulence in the solar wind. At this point we also provide suggestions for further work.

2. Problem statement and basic equations

In this paper we will be studying the interscale energy and helicity transfers that govern the dynamics of homogeneous MHD turbulence in the absence of a background magnetic field. We consider the turbulent flow to be incompressible and make no explicit assumptions about the value of the magnetic Prandtl number. The MHD equations for incompressible flow are

$$\partial_t \boldsymbol{u} = -\frac{1}{\rho}\boldsymbol{\nabla} P - (\boldsymbol{u}\cdot\boldsymbol{\nabla})\boldsymbol{u} + \frac{1}{\rho}(\boldsymbol{\nabla}\times\boldsymbol{b})\times\boldsymbol{b} + \nu\Delta\boldsymbol{u}, \tag{2.1}$$

$$\partial_t \boldsymbol{b} = (\boldsymbol{b}\cdot\boldsymbol{\nabla})\boldsymbol{u} - (\boldsymbol{u}\cdot\boldsymbol{\nabla})\boldsymbol{b} + \eta\Delta\boldsymbol{b}, \tag{2.2}$$

$$\boldsymbol{\nabla}\cdot\boldsymbol{u} = 0 \quad \text{and} \quad \boldsymbol{\nabla}\cdot\boldsymbol{b} = 0, \tag{2.3a,b}$$

where $\boldsymbol{u}$ denotes the velocity field, $\boldsymbol{b}$ the magnetic induction expressed in Alfvén units, ν the kinematic viscosity, η the magnetic resistivity, P the pressure and ρ the density, which is set to unity for convenience.

For simplicity at first we consider periodic boundary conditions on a domain $\Omega = [0, L]^3 \subset \mathbb{R}^3$, thus working with the discrete Fourier transformed MHD equations

$$\begin{aligned}(\partial_t + \nu k^2)\hat{\boldsymbol{u}}(\boldsymbol{k}) \;=\; & -FT\left[\boldsymbol{\nabla}\left(P + \frac{|\boldsymbol{u}|^2}{2}\right)\right] \\ & + \sum_{\boldsymbol{k}+\boldsymbol{p}+\boldsymbol{q}=0}\left[-(\mathrm{i}\boldsymbol{p}\times\hat{\boldsymbol{u}}(\boldsymbol{p}))^*\times\hat{\boldsymbol{u}}(\boldsymbol{q})^* + (\mathrm{i}\boldsymbol{p}\times\hat{\boldsymbol{b}}(\boldsymbol{p}))^*\times\hat{\boldsymbol{b}}(\boldsymbol{q})^*\right],\end{aligned} \tag{2.4}$$

$$(\partial_t + \eta k^2)\hat{\boldsymbol{b}}(\boldsymbol{k}) \;=\; \mathrm{i}\boldsymbol{k}\times\sum_{\boldsymbol{k}+\boldsymbol{p}+\boldsymbol{q}=0}\hat{\boldsymbol{u}}(\boldsymbol{p})^*\times\hat{\boldsymbol{b}}(\boldsymbol{q})^*, \tag{2.5}$$

where FT denotes the three-dimensional Fourier transform as a linear operator acting on $L^2(\Omega)$ functions, $\hat{\boldsymbol{u}}$ and $\hat{\boldsymbol{b}}$ denote the Fourier transforms of the velocity and magnetic fields, respectively, and the inertial term $(\boldsymbol{u}\cdot\boldsymbol{\nabla})\boldsymbol{u}$ in the momentum equation (2.1) has been written in rotational form $(\boldsymbol{u}\cdot\boldsymbol{\nabla})\boldsymbol{u} = (\boldsymbol{\nabla}\times\boldsymbol{u})\times\boldsymbol{u} + 0.5\boldsymbol{\nabla}|\boldsymbol{u}|^2$. In order to determine the contribution of specific interactions to the fluxes of magnetic helicity and magnetic energy, eventually we will formally take the limit $L\to\infty$ in § 7, necessarily assuming that the relevant functions are then well behaved at infinity to ensure the convergence of the respective Fourier integrals (a discussion of this point can be found in the book by Titchmarsh (1939)).

2.1. *Helical decomposition*

The decomposition of the Fourier transform of a solenoidal vector field in circularly polarised waves as proposed by Constantin & Majda (1988) has been used in several investigations of hydrodynamic turbulence (Waleffe 1992; Biferale *et al.* 2012; Biferale & Titi 2013) in order to establish the properties of energy transfer depending on the kinetic helicity. For conciseness we only review the fundamental properties of the helical decomposition and refer to the relevant literature for details and derivations.

The action of the curl operator on a square integrable real vector field $\boldsymbol{v}(\boldsymbol{x})$ can be viewed in spectral space as the action of a linear operator on the Fourier transform $\hat{\boldsymbol{v}}(\boldsymbol{k})$ of $\boldsymbol{v}(\boldsymbol{x})$,

$$I_k : \mathbb{C}^3 \longrightarrow \mathbb{C}^3, \tag{2.6}$$

$$\hat{\boldsymbol{v}}(\boldsymbol{k}) \longrightarrow \mathrm{i}\boldsymbol{k} \times \hat{\boldsymbol{v}}(\boldsymbol{k}). \tag{2.7}$$

As such the linear operator $I_k(\cdot) = \mathrm{i}\boldsymbol{k} \times (\cdot)$ has a set of linearly independent eigenvectors defining a basis of $\mathbb{C}^3$, thus $\hat{\boldsymbol{v}}(\boldsymbol{k})$ can be expanded in this basis. That is, it can be expressed as a linear combination of eigenvectors $\mathrm{i}\boldsymbol{k}$, $\boldsymbol{h}_+(\boldsymbol{k})$ and $\boldsymbol{h}_-(\boldsymbol{k})$ of the curl operator I_k, where

$$\mathrm{i}\boldsymbol{k} \times \boldsymbol{h}_{s_k} = s_k k \boldsymbol{h}_{s_k}, \tag{2.8}$$

$$-\mathrm{i}\boldsymbol{k} \times \boldsymbol{h}^*_{s_k} = s_k k \boldsymbol{h}^*_{s_k}, \tag{2.9}$$

$s_k = \pm 1$ and $s_k k = \pm k$ are the non-zero eigenvalues of the curl operator in spectral space and $*$ denotes the complex conjugate. (Note that the curl operator can have eigenvectors with non-zero eigenvalues, as it involves the cross product of two complex vectors. This is not necessarily orthogonal to the plane spanned by the two complex vectors, instead it is orthogonal to the plane spanned by the complex conjugates of the two vectors.) The complex eigenvectors are orthogonal to each other and are fully helical. They are normalised to unit vectors for the remainder of this paper.

Since $\hat{\boldsymbol{u}}(\boldsymbol{k})$ and $\hat{\boldsymbol{b}}(\boldsymbol{k})$ are solenoidal, they can be expressed in terms of $\boldsymbol{h}_-$, $\boldsymbol{h}_+$ only

$$\hat{\boldsymbol{u}}(\boldsymbol{k}, t) = u_-(\boldsymbol{k}, t)\boldsymbol{h}_-(\boldsymbol{k}) + u_+(\boldsymbol{k}, t)\boldsymbol{h}_+(\boldsymbol{k}) = \sum_{s_k} u_{s_k}(\boldsymbol{k}, t)\boldsymbol{h}_{s_k}(\boldsymbol{k}), \tag{2.10}$$

$$\hat{\boldsymbol{b}}(\boldsymbol{k}, t) = b_-(\boldsymbol{k}, t)\boldsymbol{h}_-(\boldsymbol{k}) + b_+(\boldsymbol{k}, t)\boldsymbol{h}_+(\boldsymbol{k}) = \sum_{s_k} b_{s_k}(\boldsymbol{k}, t)\boldsymbol{h}_{s_k}(\boldsymbol{k}), \tag{2.11}$$

where u_{s_k} and b_{s_k} are complex coefficients. These coefficients can be calculated by taking the inner product of the basis vectors with the appropriate fields

$$u_{s_k}(\boldsymbol{k}, t) = \frac{\boldsymbol{h}^*_{s_k}(\boldsymbol{k}) \cdot \boldsymbol{u}(\boldsymbol{k}, t)}{\boldsymbol{h}_{s_k}(\boldsymbol{k}) \cdot \boldsymbol{h}^*_{s_k}(\boldsymbol{k})}, \tag{2.12}$$

and

$$b_{s_k}(\boldsymbol{k}, t) = \frac{\boldsymbol{h}^*_{s_k}(\boldsymbol{k}) \cdot \boldsymbol{b}(\boldsymbol{k}, t)}{\boldsymbol{h}_{s_k}(\boldsymbol{k}) \cdot \boldsymbol{h}^*_{s_k}(\boldsymbol{k})}. \tag{2.13}$$

In order to keep the derivations concise we suppress the dependence of the coefficients on time and wavevector from now on in the notation.

The helical decomposition of a solenoidal vector field was first applied to incompressible MHD flows by Lessinnes *et al.* (2009), who derived a dynamical system in Fourier space describing helical triadic interactions in MHD. This system was subsequently used to construct a helical shell model of MHD turbulence. In the following section we briefly review the derivation carried out by Lessinnes *et al.* (2009).

3. The evolution of the helical modes

The equations describing the evolution of the helical coefficients u_{s_k} and b_{s_k} are derived by substituting the decompositions (2.10) and (2.11) into the MHD equations for incompressible flow and then taking the inner product with $\boldsymbol{h}_{s_k}$ on both sides of the respective equations. The resulting evolution equation for the helical coefficient u_{s_k} is

$$\begin{aligned}(\partial_t + \nu k^2)u_{s_k} &= \boldsymbol{h}^*_{s_k}\cdot\left(-FT\left[\nabla\left(P+\frac{|\boldsymbol{u}|^2}{2}\right)\right]\right)\\ &\quad+\boldsymbol{h}^*_{s_k}\cdot\sum_{\boldsymbol{k}+\boldsymbol{p}+\boldsymbol{q}=0}\left[-(\mathrm{i}\boldsymbol{p}\times\hat{\boldsymbol{u}}(\boldsymbol{p}))^*\times\hat{\boldsymbol{u}}(\boldsymbol{q})^*+(\mathrm{i}\boldsymbol{p}\times\hat{\boldsymbol{b}}(\boldsymbol{p}))^*\times\hat{\boldsymbol{b}}(\boldsymbol{q})^*\right]\\ &= -\frac{1}{2}\sum_{s_p,s_q}\sum_{\boldsymbol{k}+\boldsymbol{p}+\boldsymbol{q}=0}(s_pp-s_qq)\left[\boldsymbol{h}^*_{s_p}\times\boldsymbol{h}^*_{s_q}\cdot\boldsymbol{h}^*_{s_k}\right](u^*_{s_p}u^*_{s_q}-b^*_{s_p}b^*_{s_q}),\end{aligned}\tag{3.1}$$

where the dummy variables $\boldsymbol{p}$ and $\boldsymbol{q}$ were exchanged in order to symmetrise the momentum equation with respect to $\boldsymbol{p}$ and $\boldsymbol{q}$ and thus to obtain the factor $(s_pp - s_qq)/2$. Following an analogous procedure (Lessinnes *et al.* 2009) for the helical coefficient b_{s_k} of the magnetic field leads to

$$\begin{aligned}(\partial_t+\eta k^2)b_{s_k} &= \boldsymbol{h}^*_{s_k}\cdot\left[\mathrm{i}\boldsymbol{k}\times\sum_{\boldsymbol{k}+\boldsymbol{p}+\boldsymbol{q}=0}\hat{\boldsymbol{u}}(\boldsymbol{p})^*\times\hat{\boldsymbol{b}}(\boldsymbol{q})^*\right]\\ &= \frac{s_kk}{2}\sum_{s_p,s_q}\sum_{\boldsymbol{k}+\boldsymbol{p}+\boldsymbol{q}=0}\left[\boldsymbol{h}^*_{s_p}\times\boldsymbol{h}^*_{s_q}\cdot\boldsymbol{h}^*_{s_k}\right](u^*_{s_p}b^*_{s_q}-b^*_{s_p}u^*_{s_q}).\end{aligned}\tag{3.2}$$

In order to study the interaction of helical modes, that is the evolution of the helical coefficients due to the mode coupling only, the diffusivities are from now on omitted. For a given triad $\boldsymbol{k}, \boldsymbol{p}, \boldsymbol{q}$ of wavevectors, expressions for the first time derivatives of each helical coefficient are obtained from (3.1) and (3.2) and from the corresponding equations for b_{s_p}, b_{s_q}, u_{s_p} and u_{s_q}. This leads to the following system of coupled ODEs describing the evolution of the helical coefficients in a single triad interaction

$$\left.\begin{aligned}\partial_tu_{s_k} &= (s_pp-s_qq)g_{kpq}\,(u^*_{s_p}u^*_{s_q}-b^*_{s_p}b^*_{s_q}),\\ \partial_tu_{s_p} &= (s_qq-s_kk)g_{kpq}\,(u^*_{s_q}u^*_{s_k}-b^*_{s_q}b^*_{s_k}),\\ \partial_tu_{s_q} &= (s_kk-s_pp)g_{kpq}\,(u^*_{s_k}u^*_{s_p}-b^*_{s_k}b^*_{s_p}),\end{aligned}\right\}\tag{3.3}$$

$$\left.\begin{aligned}\partial_tb_{s_k} &= -s_kkg_{kpq}\,(u^*_{s_p}b^*_{s_q}-b^*_{s_p}u^*_{s_q}),\\ \partial_tb_{s_p} &= -s_ppg_{kpq}\,(u^*_{s_q}b^*_{s_k}-b^*_{s_q}u^*_{s_k}),\\ \partial_tb_{s_q} &= -s_qqg_{kpq}\,(u^*_{s_k}b^*_{s_p}-b^*_{s_k}u^*_{s_p}),\end{aligned}\right\}\tag{3.4}$$

where the geometric factor

$$g_{kpq} = -\tfrac{1}{2}\boldsymbol{h}^*_{s_p}\times\boldsymbol{h}^*_{s_q}\cdot\boldsymbol{h}^*_{s_k},\tag{3.5}$$

is introduced for conciseness, following Waleffe (1992) and Lessinnes *et al.* (2009). It can also be written as

$$g_{kpq} = \frac{s_k s_p s_q}{2} \mathrm{e}^{\mathrm{i}\alpha(k,p,q)} \frac{N}{2kpq} (s_k k + s_p p + s_q q), \tag{3.6}$$

where α is a wavenumber-dependent real number determined by the orientation of the triad and N a factor depending on the shape of the triad. Further details and a derivation of (3.6) can be found in the paper by Waleffe (1992).

The three ideal invariants, total energy, magnetic helicity and cross-helicity are defined respectively as

$$E_{tot} = \frac{1}{2} \sum_{\boldsymbol{k}} \langle |\hat{\boldsymbol{u}}(\boldsymbol{k})|^2 + |\hat{\boldsymbol{b}}(\boldsymbol{k})|^2 \rangle = \frac{1}{2} \sum_{\boldsymbol{k}, s_k} \left(\langle |u_{s_k}|^2 \rangle + \langle |b_{s_k}|^2 \rangle \right), \tag{3.7}$$

$$H_{mag} = \sum_{\boldsymbol{k}} \langle \hat{\boldsymbol{a}}(\boldsymbol{k}) \hat{\boldsymbol{b}}(-\boldsymbol{k}) \rangle = \sum_{\boldsymbol{k}, s_k} \frac{s_k}{k} \langle |b_{s_k}|^2 \rangle, \tag{3.8}$$

$$H_c = \sum_{\boldsymbol{k}} \langle \hat{\boldsymbol{u}}(\boldsymbol{k}) \hat{\boldsymbol{b}}(-\boldsymbol{k}) \rangle = \sum_{\boldsymbol{k}, s_k} \mathrm{Re} \left(\langle u_{s_k} b^*_{s_k} \rangle \right), \tag{3.9}$$

where $\boldsymbol{a}$ denotes the vector potential of the magnetic field, Re the real part of a complex number and angle brackets an ensemble average. They are conserved in single triad interactions (Lessinnes *et al.* 2009).

4. Stability of steady solutions

Examining the linear stability of steady solutions of the system (3.3)–(3.4) can reveal the influence which the helicities of the interacting modes have on the interscale transfer of a given quantity of interest.

The system (3.3) without a magnetic field (that is for $b_s = 0$) was analysed by Waleffe (1992) with respect to the linear stability of its steady solutions. Linearly unstable solutions were found depending on the helicities of the interacting modes. This result was then interpreted following the instability assumption inspired by the formal analogy to rigid-body rotation, where rotation around the axis of middle inertia is unstable. The existence of a linearly unstable solution involving a velocity field mode $\hat{\boldsymbol{u}}$ is interpreted as the $\hat{\boldsymbol{u}}$-mode losing energy to the other two modes it interacts with. An equivalent assumption had already been used by Kraichnan (1967) for two-dimensional hydrodynamic turbulence. In the remainder of this paper we take a similar approach and investigate the linear stability of steady solutions of the system (3.3)–(3.4) in view of possible applications to spectral transfer processes in MHD, and in particular, for the inverse transfers of total energy and magnetic helicity. In principle, a similar analysis could be carried out for the remaining ideal invariant, the cross-helicity.

4.1. *The steady solutions*

The system (3.3)–(3.4) of six coupled ODEs has several steady solutions that one can linearise about. To simplify the notation, a (formal) solution of the system (3.3)–(3.4) consisting of helical $\hat{\boldsymbol{u}}$- and $\hat{\boldsymbol{b}}$-field modes interacting in a given triad $\boldsymbol{k}, \boldsymbol{p}, \boldsymbol{q}$ is written as:

$$(u_{s_k}, u_{s_p}, u_{s_q}; b_{s_k}, b_{s_p}, b_{s_q}). \tag{4.1}$$

In order to find the steady solutions of the system (3.3)–(3.4), we assume (without loss of generality) that the middle components $b_{s_p} = B_{s_p}$ and $u_{s_p} = U_{s_p}$ are constant in time. Then (3.3) and (3.4) require the other four components to vanish by the following argument. A steady solution requires $\partial_t u_{s_k} = 0$, and the only way that this can happen non-trivially is if both products $u^*_{s_p} u^*_{s_q}$ and $b^*_{s_p} b^*_{s_q}$ vanish (this requires assuming that no cancellations occur. However, the occurrence of cancellations would require the system to be in a specific state, which is unlikely to happen frequently in a chaotic system). Since $u_{s_p} = U_{s_p}$ is constant in time, $u_{s_q} = 0$ and similarly $b_{s_q} = 0$. This leaves us with

$$(u_{s_k}, U_{s_p}, 0; b_{s_k}, B_{s_p}, 0). \tag{4.2}$$

Applying the same argument to $\partial_t u_{s_q}$, it follows that u_{s_k} and b_{s_k} must also vanish. Therefore a steady solution of the system (3.3)–(3.4) has the form

$$(0, U_{s_p}, 0; 0, B_{s_p}, 0). \tag{4.3}$$

It can now be checked for consistency that $\partial_t b_s = 0$ for k, p and q also. Therefore the solution is steady for the magnetic field and for the velocity field alike. Asides from the just explained example, steady solutions of the form $(U_{s_k}, 0, 0; B_{s_k}, 0, 0)$ and $(0, 0, U_{s_q}; 0, 0, B_{s_q})$ are obtained in the same way.

Thus the steady solutions of (3.3)–(3.4) are of the same form as for the hydrodynamic case (Waleffe 1992), where at least two of the three interacting modes vanish. However, there are two special cases: one where the magnetic field component B_s also vanishes, while $U_s \neq 0$ and the other, where the velocity field component U_s vanishes, while $B_s \neq 0$. The former case may perhaps be connected to a dynamo process. At this point we note that for the kinematic dynamo, where the back reaction of the magnetic field on the velocity field can be neglected, the (linear) stability of the velocity field coefficients u_s is only determined by hydrodynamic interactions. We will come back to this point in § 8.

4.2. *Linear stability analysis*

In order to assess whether a given steady solution is linearly stable in our particular setting, we assume without loss of generality that the coefficients u_{s_p} and b_{s_p} corresponding to wavevector $\boldsymbol{p}$ are non-zero and constant in time, that is, we study the linear stability of the solution $(0, U_{s_p}, 0; 0, B_{s_p}, 0)$ with respect to infinitesimal perturbations of the four modes that had been set to zero. As the first-order equations involve the coupling of all three modes of a given triad, little information can be obtained from them at first sight. Therefore we pass to second-order time derivatives of the evolution equations for the perturbations u_{s_k}, b_{s_k}, u_{s_q} and b_{s_q}. Taking time derivatives on both sides of (3.3)–(3.4) and subsequently substituting any occurrence of a first-order time derivative on the right-hand side by the appropriate evolution equation, we obtain

$$\begin{aligned}
\partial_t^2 u_{s_k} &= |g_{kpq}|^2 (s_p p - s_q q)\left[\left((s_k k - s_p p)|U_{s_p}|^2 + s_q q\,|B_{s_p}|^2\right) u_{s_k}\right] \\
&\quad - |g_{kpq}|^2 (s_p p - s_q q)[((s_k k - s_p p) U^*_{s_p} B_{s_p} + s_q q\, U_{s_p} B^*_{s_p}) b_{s_k}], \qquad (4.4)\\
\partial_t^2 b_{s_k} &= |g_{kpq}|^2 s_k k[(s_q q\, U^*_{s_p} B_{s_p} + (s_k k - s_p p) U_{s_p} B^*_{s_p}) u_{s_k}] \\
&\quad - |g_{kpq}|^2 s_k k\left[\left(s_q q\,|U_{s_p}|^2 + (s_k k - s_p p)|B_{s_p}|^2\right) b_{s_k}\right], \qquad (4.5)
\end{aligned}$$

where terms of second order in small quantities (such as e.g. u_s^2) have been neglected. Note that these equations do not depend on modes at wavenumber q. The evolution

equations of the helical coefficients u_{s_q} and b_{s_q} can be obtained similarly and show no dependence on k, therefore we restrict our attention to the evolution of u_{s_k} and b_{s_k}.

The system (4.4) and (4.5) can be written as a matrix ODE

$$\ddot{\boldsymbol{x}} = \begin{pmatrix} \alpha & \beta \\ \gamma & \delta \end{pmatrix} \boldsymbol{x}, \tag{4.6}$$

where $\boldsymbol{x} \equiv (u_{s_k}, b_{s_k})$ and the matrix elements are

$$\alpha = |g_{kpq}|^2 (s_p p - s_q q)\left[(s_k k - s_p p)|U_{s_p}|^2 + s_q q\,|B_{s_p}|^2\right], \tag{4.7}$$

$$\beta = -|g_{kpq}|^2 (s_p p - s_q q)\left[(s_k k - s_p p) U^*_{s_p} B_{s_p} + s_q q\, U_{s_p} B^*_{s_p}\right], \tag{4.8}$$

$$\gamma = |g_{kpq}|^2 s_k k\left[s_q q\, U^*_{s_p} B_{s_p} + (s_k k - s_p p) U_{s_p} B^*_{s_p}\right], \tag{4.9}$$

$$\delta = -|g_{kpq}|^2 s_k k\left[s_q q\,|U_{s_p}|^2 + (s_k k - s_p p)|B_{s_p}|^2\right]. \tag{4.10}$$

The linear stability of this system can be determined from the eigenvalues λ_1 and λ_2 of the matrix in (4.6). These eigenvalues depend not only on the helicities of the interacting modes and on the magnitudes of U_{s_p} and B_{s_p} relative to each other, but also on the alignment between the magnetic and velocity field modes at wavevector $\boldsymbol{p}$, that is, on the cross-helicity. For a given steady solution to be unstable the perturbations have to be exponentially growing, and so at least for one of the eigenvalues, $\sqrt{\lambda_i}$ (for $i = 1, 2$) must have a positive real part. We will now assess under which conditions this is possible.

The eigenvalues λ_i $(i = 1, 2)$ are given by

$$\lambda_{1,2} = \frac{\alpha + \delta}{2} \pm \sqrt{\frac{(\alpha + \delta)^2}{4} - \alpha\delta + \beta\gamma}. \tag{4.11}$$

For convenience we define

$$x \equiv \frac{\alpha + \delta}{2} \quad \text{and} \quad Q \equiv \alpha\delta - \beta\gamma, \tag{4.10a,b}$$

such that

$$\begin{aligned} x = &-\frac{|g_{kpq}|^2}{2}|U_{s_p}|^2[s_k k s_q q + (s_k k - s_p p)(s_q q - s_p p)] \\ &-\frac{|g_{kpq}|^2}{2}|B_{s_p}|^2[s_k k(s_k k - s_p p) + s_q q(s_q q - s_p p)], \end{aligned} \tag{4.13}$$

and

$$Q = |g_{kpq}|^4 s_k k s_q q (s_k k - s_p p)(s_q q - s_p p)((|U_{s_p}|^2 + |B_{s_p}|^2)^2 - 4H_c(p)^2), \tag{4.14}$$

hence the cross-helicity $H_c(p)$ enters the dynamics through the parameter Q. The derivation of (4.14) can be found in appendix A. Note that the term $|U_{s_p}|^4 + |B_{s_p}|^4 + 2|U_{s_p}|^2|B_{s_p}|^2 - 4H_c(p)^2$ is always positive, regardless of the value of H_c since $|H_c(p)| \leqslant |U_{s_p}||B_{s_p}|$, thus the sign of Q is determined by the helicities of the interacting modes and the wavenumber ordering.

The eigenvalues λ_i can now be written more concisely as

$$\lambda_{1,2} = x \pm \sqrt{x^2 - Q}, \tag{4.15}$$

therefore the possibility of finding exponential solutions of the system (4.6) depends on the values of x and Q. Apart from the trivial case, where $x = 0$ and $Q = 0$, there is only one case for which no linear instability occurs: this is if $x < 0$ and $|x| > |\sqrt{x^2 - Q}|$, since then $\sqrt{\lambda_1}$ and $\sqrt{\lambda_2}$ are imaginary numbers allowing only oscillatory solutions of the matrix ODE (4.6). All other cases lead to exponentially growing, as well as exponentially decaying, solutions.

Cases in which $x > 0$ and $Q < 0$ result in the largest eigenvalues and thus in the fastest growing exponential solution. These cases are therefore of special interest, as within the framework of the instability assumption they may lead to the largest energy transfer and thus can yield information about which combination of parameters facilitates most of the energy and helicity transfers. We will consider related points in further detail in §§ 7 and 8.

As can be seen from the structure of the terms x and Q, the relative magnitudes and the ordering of the wavenumbers in a given triad will influence the stability of steady solutions. In view of the continuous interest in non-locality of interactions in MHD turbulence (Brandenburg 2001; Alexakis *et al.* 2005; Debliquy *et al.* 2005; Cho 2010; Müller *et al.* 2012), we point towards specific results for local and non-local interactions where appropriate. Following Waleffe (1992), for wavenumbers ordered $k < p < q$, the non-local limit is defined as $k \ll p \simeq q$, while local interactions are characterised by $k \simeq p \simeq q$.

5. Instability and helical interactions

Since $s = \pm 1$, interactions between helical modes which all have helicities of opposite signs are not possible, and at least two modes will always have helicities of the same sign. Therefore we have four classes of possible helicity combinations

$$s_k = s_p \neq s_q, \quad s_k = s_q \neq s_p, \quad s_k \neq s_q = s_p \quad \text{and} \quad s_k = s_q = s_p, \tag{5.1a–d}$$

each of which occurs twice as s can take the values ± 1. These four possible (classes of) combinations are now studied on a case-by-case approach in order to determine when a certain combination of helicities leads to exponentially growing solutions of the system (4.6).

5.1. *The case* $s_k = s_q \neq s_p$

Since the expressions in square brackets of (4.13) become

$$kq + (k+p)(q+p) > 0 \quad \text{and} \quad k(k+p) + q(q+p) > 0, \tag{5.2a,b}$$

one obtains $x = (\alpha + \delta)/2 < 0$. For an unstable solution $|x| < |\sqrt{x^2 - Q}|$, however, we obtain $Q > 0$ since

$$Q \sim s_k s_q kq(s_k k - s_p p)(s_q q - s_p p), \tag{5.3}$$

which is positive for $s_k = s_q \neq s_p$. Furthermore we obtain $Q < x^2$ (see appendix B) and thus $|x| > |\sqrt{x^2 - Q}|$, which results in negative eigenvalues of the matrix in (4.6). Therefore we do not obtain unstable solutions for the case $s_k = s_q \neq s_p$, and this is independent of the ordering of the wavenumbers k, p and q. Note that this implies that exponentially growing solutions of (4.6) are impossible if the perturbations u_{s_k}, u_{s_q}, b_{s_k} and b_{s_q} have helicities opposite to the helicities of the modes U_{s_p} and B_{s_p} constituting the steady solution.

For the remaining helicity combinations, which do result in unstable solutions, the ordering of wavenumbers matters. The arguments used to decide whether or not an exponentially growing solution becomes possible are similar to the procedure employed for the case $s_k = s_q \neq s_p$ described above.

5.2. *The case* $s_k \neq s_p = s_q$

In this case we obtain

$$Q \sim kq(k+p)(q-p), \tag{5.4}$$

and

$$x = -\frac{|g_{kpq}|^2}{2}|U_{s_p}|^2[-kq-(k+p)(q-p)] - \frac{|g_{kpq}|^2}{2}|B_{s_p}|^2[k(k+p)+q(q-p)]. \tag{5.5}$$

The stability of a steady solution depends on the signs of these terms which in turn depend on wavenumber ordering, cross-helicity and the ratio $|U_{s_p}|/|B_{s_p}|$.

(1) For $k<p<q$ we obtain unstable solutions if $|U_{s_p}| \gtrapprox |B_{s_p}|$, since then $x>0$. For $|B_{s_p}|>|U_{s_p}|$ unstable solutions are still possible, provided $H_c(p)$ is small and $|B_{s_p}|$ not much larger than $|U_{s_p}|$. Thus in regions of large cross-helicity unstable solutions only occur for weak magnetic fields. The method by which these results are obtained is explained in appendix C.

For non-local interactions ($k \ll p \simeq q$) we obtain $Q=0$ and the sign of x determines whether unstable solutions occur. The term x is now of the form

$$x \simeq \frac{|g_{kpq}|^2}{2}kq(|U_{s_p}|^2 - |B_{s_p}|^2), \tag{5.6}$$

hence non-local interactions lead to unstable solutions if $|B_{s_p}|<|U_{s_p}|$.

(2) For $k<q<p$, Q will become negative, leading to unstable solutions regardless of the ratio $|U_{s_p}|/|B_{s_p}|$ and the value of $H_c(p)$.

(3) For $p<k<q$ again we obtain unstable solutions if $|U_{s_p}| \gtrapprox |B_{s_p}|$, since then $x>0$. For $|B_{s_p}|>|U_{s_p}|$ unstable solutions are still possible, provided $H_c(p)$ is small and $|B_{s_p}|/|U_{s_p}|$ not $\gg 1$ (see appendix C). Non-local interactions ($p \ll k \simeq q$) lead to unstable solutions if $|U_{s_p}|>|B_{s_p}|$, because then

$$x \simeq |g_{kpq}|^2k^2(|U_{s_p}|^2 - |B_{s_p}|^2) > 0. \tag{5.7}$$

In summary, a given steady solution in this case is more likely to be stable if the non-zero mode is at medium or low wavenumbers in regions of high cross-helicity.

5.3. *The case* $s_k = s_p = s_q$

In this case we obtain

$$Q \sim kq(k-p)(q-p), \tag{5.8}$$

and

$$x = -\frac{|g_{kpq}|^2}{2}|U_{s_p}|^2[kq+(k-p)(q-p)] - \frac{|g_{kpq}|^2}{2}|B_{s_p}|^2[k(k-p)+q(q-p)]. \tag{5.9}$$

(1) For $k<p<q$ we obtain $Q<0$ and thus $x+\sqrt{x^2-Q} \geqslant 0$, leading to exponentially growing solutions independent of $H_c(p)$ and the ratio $|U_{s_p}|/|B_{s_p}|$. We note that both velocity and magnetic field modes have positive and negative contributions to the sign of x. This is of interest since if $x>0$ the resulting eigenvalue would be larger and thus the solution would grow faster. However, in this case this cannot be determined from the ratio $|U_{s_p}|/|B_{s_p}|$ and thus there is little information about what contributes to a faster growing exponential and thus to a more unstable solution.

For both local ($k \simeq p \simeq q$) and non-local ($k \ll p \simeq q$) interactions we obtain $Q = 0$ and the sign of x determines whether unstable solutions occur. For the non-local case only the magnetic field term is positive, and x has the form

$$x \simeq \frac{|g_{kpq}|^2}{2} kq(|B_{s_p}|^2 - |U_{s_p}|^2) \tag{5.10}$$

leading to unstable solutions if $|B_{s_p}| > |U_{s_p}|$, while for local interactions no instability occurs as the only term in x that does not vanish is $-|g_{kpq}|^2|U_{s_p}|^2 kq < 0$.

(2) For $k < q < p$, the possibility of exponentially growing solutions depends on the ratio $|U_{s_p}|/|B_{s_p}|$ and on the relative magnitudes of the wavenumbers k, p and q, as now $Q > 0$. Since the magnetic field term in x is now positive, instabilities occur for $|U_{s_p}|/|B_{s_p}| < 1$. If $|U_{s_p}|/|B_{s_p}| > 1$ it depends also on the cross-helicity whether instabilities occur. For maximal $H_c(p)$ we obtain $x^2 - Q > 0$, hence the solutions will be stable. If $H_c(p) = 0$ and $|U_{s_p}|/|B_{s_p}|$ is not too small, instabilities will occur, depending also on the shape of the triad (see appendix C for further details). In general, the smaller $|U_{s_p}|/|B_{s_p}|$ the more unstable is the solution.

(3) For $p < k < q$ we obtain $x < 0$ and $Q > 0$, furthermore $x^2 - Q > 0$ independent of $|U_{s_p}|/|B_{s_p}|$ and $H_c(p)$ (see appendix B), thus no unstable solutions occur. Non-local interactions ($p \ll k \simeq q$) do not lead to unstable solutions, since

$$x \simeq -|g_{kpq}|^2[k^2 - kp](|U_{s_p}|^2 + |B_{s_p}|^2) < 0. \tag{5.11}$$

5.4. *The case* $s_k = s_p \neq s_q$

The terms determining the stability in this case are

$$Q \sim kq(k-p)(q+p), \tag{5.12}$$

and

$$x = -\frac{|g_{kpq}|^2}{2}|U_{s_p}|^2[-kq - (k-p)(q+p)] - \frac{|g_{kpq}|^2}{2}|B_{s_p}|^2[k(k-p) + q(q+p)]. \tag{5.13}$$

(1) For $k < p < q$ unstable solutions occur independent of the ratio $|U_{s_p}|/|B_{s_p}|$, and since both magnetic and velocity field terms have positive and negative contributions to the sign of x, we are in a similar situation to the previous case. However, in the present case $Q \simeq 0$ only for local ($k \simeq p \simeq q$) interactions. It is now the velocity field term $|g_{kpq}|^2|U_{s_p}|^2 kq > 0$ which ensures that exponentially growing solutions exist for local interactions provided $|U_{s_p}| > 2|B_{s_p}|$.

(2) For $k < q < p$ the result is the same, since reversing the relative ordering of p and q does not change the sign of Q. That is, exponentially growing solutions occur.

(3) For $p < k < q$ the term Q is positive and the term proportional to $|U_{s_p}|^2$ is positive while the term proportional to $|B_{s_p}|^2$ is negative. Thus instabilities occur if $|U_{s_p}|/|B_{s_p}| \gtrapprox 1$. For $|U_{s_p}|/|B_{s_p}| < 1$ the occurrence of instabilities depends on the value of $H_c(p)$. If $H_c(p)$ is maximal and magnetic and velocity field are fully aligned, then the solutions are stable. For zero cross-helicity and $|B_{s_p}|$ being not much larger than $|U_{s_p}|$, solutions are unstable (see appendix C).

This type of helicity combination is another possibility for non-local interactions of the type $p \ll k \simeq q$ leading to exponentially growing solutions if $|U_{s_p}| > |B_{s_p}|$, since then

$$x \simeq |g_{kpq}|^2 k^2(|U_{s_p}|^2 - |B_{s_p}|^2) > 0. \tag{5.14}$$

The results of the dependence of the occurrence of unstable solutions on combinations of helicities, wavenumber ordering, relative magnitudes of the $\boldsymbol{u}$ and $\boldsymbol{b}$ modes and cross-helicities at wavenumber p are summarised in tables 1–3.

Helicities	H_c	Constraint	Stability
$s_k \neq s_q = s_p$	n/a	$\lvert U_{s_p}\rvert/\lvert B_{s_p}\rvert \gtrapprox 1$	Unstable
	Max	$\lvert B_{s_p}\rvert > \lvert U_{s_p}\rvert$	Stable
	0	$\lvert B_{s_p}\rvert/\lvert U_{s_p}\rvert$ not $\gg 1$	Unstable
$s_k = s_p \neq s_q$	n/a	n/a	Unstable
$s_k = s_q = s_p$	n/a	n/a	Unstable

TABLE 1. Summary of possible unstable solutions for the middle wavenumber modes $k < p < q$.

Helicities	H_c	Constraint	Stability
$s_k \neq s_q = s_p$	n/a	n/a	Unstable
$s_k = s_p \neq s_q$	n/a	n/a	Unstable
$s_k = s_q = s_p$	n/a	$\lvert B_{s_p}\rvert > \lvert U_{s_p}\rvert$	Unstable
	Max	$\lvert U_{s_p}\rvert > \lvert B_{s_p}\rvert$	Stable
	0	$\lvert U_{s_p}\rvert/\lvert B_{s_p}\rvert$ not $\gg 1$	Unstable

TABLE 2. Summary of possible unstable solutions for the largest wavenumber modes $k < q < p$.

Helicities	H_c	Constraint	Stability
$s_k \neq s_q = s_p$	n/a	$\lvert U_{s_p}\rvert/\lvert B_{s_p}\rvert \gtrapprox 1$	Unstable
	Max	$\lvert B_{s_p}\rvert > \lvert U_{s_p}\rvert$	Stable
	0	$\lvert B_{s_p}\rvert/\lvert U_{s_p}\rvert$ not $\gg 1$	Unstable
$s_k = s_p \neq s_q$	n/a	$\lvert U_{s_p}\rvert/\lvert B_{s_p}\rvert \gtrapprox 1$	Unstable
	Max	$\lvert B_{s_p}\rvert > \lvert U_{s_p}\rvert$	Stable
	0	$\lvert B_{s_p}\rvert/\lvert U_{s_p}\rvert$ not $\gg 1$	Unstable
$s_k = s_q = s_p$	n/a	n/a	Stable

TABLE 3. Summary of possible unstable solutions for the smallest wavenumber modes $p < k < q$.

6. Energy transfers and the instability assumption

In order to use the results of the previous section to derive results for the transfers of the ideal invariants total energy E_{tot} and magnetic helicity H_{mag}, we invoke the instability assumption (Waleffe 1992). Generalised to MHD turbulence, this assumption asserts that energy is transferred away from modes whose evolution equation for the helicity coefficient is linearly unstable, into the other two modes it is coupled to by a triad interaction given through the system (3.3)–(3.4).

Therefore the results of the stability analysis determine whether a given helicity combination mainly contributes to forward or reverse transfer of energy. That is, if a steady solution at wavenumber p is unstable and energy is transferred away from B_{s_p} and U_{s_p} into the modes they interact with (note that B_{s_p} and U_{s_p} do not interact with each other directly), then the wavenumber ordering $k < q < p$ results in reverse

transfer of energy, while $p < k < q$ results in forward transfer and $k < p < q$ in a split transfer with contributions to forward and reverse directions of energy transfer.

Several immediate results can be deduced from the summary of the stability analysis for the different helicity combinations presented in tables 1–3. First, unlike in non-conducting fluids modes, corresponding to the largest wavenumber in a given triad can be unstable, leading to more possibilities for reverse spectral energy transfer in MHD compared to hydrodynamics. Second, all three helicities influence the direction of energy transfers, and reverse transfers are also possible for cases of unlike helicities. Third, forward transfers appear to be more quenched in regions of high cross-helicity than reverse transfers. Fourth, very non-local triads contribute mainly to reverse transfers in magnetically dominated systems through interactions of modes with like helicity. They only contribute to forward transfers through interactions of modes with unlike helicity and mostly if the kinetic energy is larger than the magnetic energy.

Therefore we obtain that reverse spectral transfer becomes much more likely in MHD turbulence than in turbulence of non-conducting fluids, which reflects the predictions from absolute equilibrium spectra (Frisch *et al.* 1975; Zhu, Yang & Zhu 2014) and the well-established numerical results on inverse cascades, and more generally reverse transfer, in MHD turbulence (Pouquet *et al.* 1976; Pouquet & Patterson 1978; Balsara & Pouquet 1999; Brandenburg 2001; Alexakis *et al.* 2006; Müller *et al.* 2012; Berera & Linkmann 2014; Brandenburg *et al.* 2015).

We note that the transfer directions deduced so far may or may not contribute to forward and inverse cascades of energy and magnetic helicity, as no information on the constancy, or otherwise, of the fluxes of these quantities through a given wavenumber is available at this point. The aim of the next section is to determine the contribution of the individual transfers to energy and magnetic helicity cascades.

7. Transfer and cascades of total energy and magnetic helicity

In order to determine the contribution of a given interaction of helical modes to energy and magnetic helicity cascades, the fluxes of these quantities need to be calculated and studied in the respective inertial ranges where they are wavenumber independent. However, several technical details need to be discussed before we can proceed to this calculation.

In the discrete Fourier representation the evolution equations of the kinetic and magnetic energy spectra $E_{kin}(k)$ and $E_{mag}(k)$ are obtained by multiplying the relevant equations in the system (3.3) by $u^*_{s_k}$ and $b^*_{s_k}$, respectively, then summing over all triads and helicity combinations and finally carrying out shell and ensemble averages. For the kinetic energy spectrum this leads to

$$\partial_t E_{kin}(k) = \frac{1}{2}\sum_{p,q}^{\Delta}\sum_{i=1}^{8}(t^{(i)}_{HD}(k,p,q) + t^{(i)}_{LF}(k,p,q)), \tag{7.1}$$

where $\sum_{p,q}^{\Delta}$ denotes a sum over all wavenumbers p and q whose wavevectors $\boldsymbol{p}$ and $\boldsymbol{q}$ form a triad with $\boldsymbol{k}$ such that $\boldsymbol{k}+\boldsymbol{p}+\boldsymbol{q}=0$ and the superscript (i) labels the eight possible helicity combinations. The transfer terms in this equation are given by

$$t^{(i)}_{HD}(k,p,q) = (s_p p - s_q q)\sum_{S(k,p,q)} g_{kpq}\langle u_{s_k} U_{s_p} u_{s_q}\rangle + \text{c.c.}, \tag{7.2}$$

and

$$t^{(i)}_{LF}(k,p,q) = -(s_p p - s_q q) \sum_{S(k,p,q)} g_{kpq} \langle u_{s_k} B_{s_p} b_{s_q} \rangle + \text{c.c.}, \tag{7.3}$$

where $S(k,p,q)$ indicates a summation over all wavevectors in shells of radius k, p and q and c.c. denotes the complex conjugate. Homogeneity allows the summation over the shells without explicitly restricting the sum to wavevectors satisfying $\boldsymbol{k}+\boldsymbol{p}+\boldsymbol{q}=0$, since triple correlations with $\boldsymbol{k}+\boldsymbol{p}+\boldsymbol{q}\neq 0$ vanish for homogeneous MHD as shown in appendix D. For the magnetic energy spectrum one obtains

$$\partial_t E_{mag}(k) = \frac{1}{2} \sum_{p,q}^{\Delta} \sum_{i=1}^{8} t^{(i)}_{mag}(k,p,q), \tag{7.4}$$

where

$$t^{(i)}_{mag}(k,p,q) = -s_k k \sum_{S(k,p,q)} g_{kpq} \langle b_{s_k} B_{s_p} u_{s_q} - b_{s_k} U_{s_p} b_{s_q} \rangle + \text{c.c.} \tag{7.5}$$

The evolution equation for the total energy spectrum $E(k) = E_{kin}(k) + E_{mag}(k)$ is given by the sum of the respective evolution equations for $E_{kin}(k)$ and $E_{mag}(k)$

$$\partial_t E(k) = \frac{1}{2} \sum_{p,q}^{\Delta} \sum_{i=1}^{8} t^{(i)}(k,p,q), \tag{7.6}$$

and total energy transfer term $t^{(i)}(k,p,q)$ therefore consists of three types of transfers

$$t^{(i)}(k,p,q) = t^{(i)}_{HD}(k,p,q) + t^{(i)}_{LF}(k,p,q) + t^{(i)}_{mag}(k,p,q). \tag{7.7}$$

The term $t^{(i)}_{HD}(k,p,q)$ denotes purely hydrodynamic transfer due to the coupling of the velocity field to itself, $t^{(i)}_{LF}(k,p,q)$ the contribution due to the Lorentz force acting on the fluid and $t^{(i)}_{mag}(k,p,q)$ the contributions due to advection of the magnetic field by the flow and conversion of kinetic to magnetic energy, that is, due to dynamo action. In real space the nonlinear term $\boldsymbol{\nabla}\times(\boldsymbol{u}\times\boldsymbol{b})$ corresponding to the magnetic transfer term can be split into an advective term $(\boldsymbol{u}\cdot\boldsymbol{\nabla})\boldsymbol{b}$ and a dynamo term $(\boldsymbol{b}\cdot\boldsymbol{\nabla})\boldsymbol{u}$, however, this splitting is obscured in Fourier space.

These terms are still written in the discrete Fourier representation of the magnetic and velocity fields. However, the calculation of the energy and magnetic helicity fluxes requires a continuous Fourier representation. The continuous transfer terms are given in terms of Fourier integrals and can formally be obtained by taking the period L to infinity, assuming that the respective integrals are well defined. The sums then become integrals and the continuous counterpart of e.g. the hydrodynamic transfer term $t^{(i)}_{HD}$ becomes

$$\begin{aligned} T^{(i)}_{HD}(k,p,q)\,\mathrm{d}k\,\mathrm{d}p\,\mathrm{d}q &= \lim_{L\to\infty} t^{(i)}_{HD}(k,p,q) \\ &= (s_p p - s_q q) \int_{|\boldsymbol{k}|=k} \mathrm{d}\boldsymbol{k} \int_{|\boldsymbol{p}|=p} \mathrm{d}\boldsymbol{p} \int_{|\boldsymbol{q}|=q} \mathrm{d}\boldsymbol{q}\, g_{kpq} \langle u_{s_k} U_{s_p} u_{s_q} \rangle + \text{c.c.} \end{aligned} \tag{7.8}$$

The transfer terms $T^{(i)}_{LF}$ and $T^{(i)}_{mag}$ are defined analogously.

7.1. *Total energy transfer*

In the absence of dissipation the total energy is conserved and the transfer term $T(k, p, q)$ in the spectral evolution equation of the total energy redistributes energy between the Fourier modes and vanishes if integrated over all space. Therefore the flux of total energy through wavenumber k due to a given interaction (i),

$$\Pi^{(i)}(k) = -\int_0^k \mathrm{d}k' \int_k^\infty \int_k^\infty T^{(i)}(k', p, q)\,\mathrm{d}p\,\mathrm{d}q, \tag{7.9}$$

can be written as the sum of two contributions: the flux of total energy into all modes at wavenumber k' due to triads with $p, q < k < k'$ minus the flux of total energy into all modes at k' due to triads with $k' < k < p, q$

$$\Pi^{(i)}(k) = \frac{1}{2}\int_k^\infty \mathrm{d}k' \int_0^k \int_0^k T^{(i)}(k', p, q)\,\mathrm{d}p\,\mathrm{d}q - \frac{1}{2}\int_0^k \mathrm{d}k' \int_k^\infty \int_k^\infty T^{(i)}(k', p, q)\,\mathrm{d}p\,\mathrm{d}q. \tag{7.10}$$

We now follow the procedure introduced by Waleffe (1992) in order to render the two integrals in (7.10) independent of k. This is achieved using a scaling argument, where the two integrals are treated separately. For conciseness we only outline the procedure briefly for the first integral on the right-hand side of (7.10) and refer to the original work of Waleffe (1992) for the full derivation. The aim is to express the transfer function in the first integral on the right-hand side of (7.10) in terms of new variables

$$v = \frac{q}{p}, \quad w = \frac{k'}{p}, \quad u = \frac{k}{p}, \tag{7.11a–c}$$

in order to remove k from the integration limits. Since $T^{(i)}_{HD}(k', p, q)$ may scale differently compared to $T^{(i)}_{LF}(k', p, q)$ and $T^{(i)}_{mag}(k', p, q)$, the term $T^{(i)}(k', p, q)$ in (7.10) must be replaced by the individual transfer terms. The transfer terms are now expressed individually in terms of the new variables u, v and w

$$T^{(i)}_{HD}(k', p, q) = p^{-\beta} T^{(i)}_{HD}(w, 1, v) = \left(\frac{k}{u}\right)^{-\beta} T^{(i)}_{HD}(w, 1, v), \tag{7.12}$$

$$T^{(i)}_{LF}(k', p, q) = p^{-\beta'} T^{(i)}_{LF}(w, 1, v) = \left(\frac{k}{u}\right)^{-\beta'} T^{(i)}_{LF}(w, 1, v), \tag{7.13}$$

and

$$T^{(i)}_{mag}(k', p, q) = p^{-\beta'} T^{(i)}_{mag}(w, 1, v) = \left(\frac{k}{u}\right)^{-\beta'} T^{(i)}_{mag}(w, 1, v), \tag{7.14}$$

where β is related to the exponent of the kinetic energy spectrum provided it has a power-law dependence on k, while the exponent β' is related to the exponents of the kinetic and magnetic energy spectra as explained in further detail in appendix E. We point out that it order to write down (7.12)–(7.14) we assumed both the magnetic energy spectrum and the kinetic energy spectrum to display power-law scaling in the inertial range. This assumption is made solely to allow estimates of the direction of

the flux. The first term on the right-hand side of (7.10) then becomes

$$\begin{aligned}
&\frac{1}{2}\int_k^\infty \mathrm{d}k' \int_0^k \int_0^k T^{(i)}(k', p, q)\,\mathrm{d}p\,\mathrm{d}q \\
&\quad = k^{3-\beta}\int_0^1 \mathrm{d}v \int_1^{1+v} \mathrm{d}w \int_1^w \mathrm{d}u \left(\frac{1}{u}\right)^{4-\beta} T^{(i)}_{HD}(w, 1, v) \\
&\qquad + k^{3-\beta'}\int_0^1 \mathrm{d}v \int_1^{1+v} \mathrm{d}w \int_1^w \mathrm{d}u \left(\frac{1}{u}\right)^{4-\beta'} \left[T^{(i)}_{LF}(w, 1, v) + T^{(i)}_{mag}(w, 1, v)\right]. \quad (7.15)
\end{aligned}$$

The second term on the right-hand side of (7.10) can be treated similarly (Waleffe 1992), and we obtain

$$\begin{aligned}
&\frac{1}{2}\int_0^k \mathrm{d}k' \int_k^\infty \int_k^\infty T^{(i)}(k', p, q)\,\mathrm{d}p\,\mathrm{d}q \\
&\quad = k^{3-\beta}\int_0^1 \mathrm{d}v \int_1^{1+v} \mathrm{d}w \int_v^1 \mathrm{d}u \left(\frac{1}{u}\right)^{4-\beta} T^{(i)}_{HD}(v, 1, w) \\
&\qquad + k^{3-\beta'}\int_0^1 \mathrm{d}v \int_1^{1+v} \mathrm{d}w \int_v^1 \mathrm{d}u \left(\frac{1}{u}\right)^{4-\beta'} \left[T^{(i)}_{LF}(v, 1, w) + T^{(i)}_{mag}(v, 1, w)\right]. \quad (7.16)
\end{aligned}$$

Combining the two results and integrating over u leads to the following expression for the total energy transfer flux

$$\begin{aligned}
\Pi^{(i)}(k) &= k^{3-\beta}\int_0^1 \mathrm{d}v \int_1^{1+v} \mathrm{d}w \left(T^{(i)}_{HD}(w, 1, v)\left[\frac{w^{\beta-3}-1}{\beta-3}\right] + T^{(i)}_{HD}(v, 1, w)\left[\frac{v^{\beta-3}-1}{\beta-3}\right]\right) \\
&+ k^{3-\beta'}\int_0^1 \mathrm{d}v \int_1^{1+v} \mathrm{d}w \left(T^{(i)}_{LF}(w, 1, v)\left[\frac{w^{\beta'-3}-1}{\beta'-3}\right] + T^{(i)}_{LF}(v, 1, w)\left[\frac{v^{\beta'-3}-1}{\beta'-3}\right]\right) \\
&+ k^{3-\beta'}\int_0^1 \mathrm{d}v \int_1^{1+v} \mathrm{d}w \left(T^{(i)}_{mag}(w, 1, v)\left[\frac{w^{\beta'-3}-1}{\beta'-3}\right] + T^{(i)}_{mag}(v, 1, w)\left[\frac{v^{\beta'-3}-1}{\beta'-3}\right]\right), \quad (7.17)
\end{aligned}$$

where $0 \leqslant v \leqslant 1 \leqslant w \leqslant 1+v$ due to the triad geometry. This now enables us to study the contribution to the total energy transfer from a given interaction (i), where the scaling of the magnetic and kinetic energy spectra will influence the transfer through the exponents β and β'. In the inertial range of total energy the energy transfer flux through a given wavenumber k does not depend on that wavenumber, which leads to the characteristic values of the scaling exponents $\beta' = \beta = 3$, making the split of the total energy transfer term into its individual components redundant in this wavenumber range. In § 7.3.1 we concentrate on the contributions of the different interactions to transfers in the inertial range of total energy and set $\beta = 3$, thus taking into account only the region in wavenumber space where this scaling is established. Since the values of β and β' may influence the direction of energy transfer, a similar approach may be useful to calculate energy and helicity transfer at the very low wavenumbers. However, this awaits consensus on the low-wavenumber scaling of the magnetic and kinetic energy spectra. Furthermore, the integrals must be cut off at some wavenumber such that a single scaling exponent for the wavenumber range of interest can be studied. As the extent of the inertial range will grow with increasing

Reynolds number, contributions from the production and dissipation ranges can safely be neglected, as they will become very small compared to the extent of the inertial range. However, in the low-wavenumber region, this argument is not applicable and further work is necessary in order to establish if very non-local interactions contribute significantly to the transfers of magnetic energy and helicity in the low-wavenumber range or not.

7.2. *Magnetic helicity transfer*

Using the decomposition into helical modes, the transfer term in the evolution equation of the magnetic helicity can be expressed through the transfer term in the evolution equation of the magnetic energy, that is

$$T_H^{(i)}(k,p,q) = \frac{s_k}{k} T_{mag}^{(i)}(k,p,q), \tag{7.18}$$

and only the transfer term which originates from the induction equation is present, since H_{mag} is a purely magnetic quantity and as such only implicitly depends on the evolution of the velocity field.

Since the magnetic helicity is an ideal invariant, the transfer term in the spectral evolution equation of the magnetic helicity vanishes if integrated over all space, therefore, similar to the flux of total energy, the flux of magnetic helicity through wavenumber k due to a given interaction (i),

$$\Pi_H^{(i)}(k) = -\int_0^k \frac{s_{k'}}{k'}\,\mathrm{d}k' \int_k^\infty \int_k^\infty T_{mag}^{(i)}(k',p,q)\,\mathrm{d}p\,\mathrm{d}q, \tag{7.19}$$

can be written as the sum of two contributions

$$\begin{aligned}\Pi_H^{(i)}(k) \;=\; & \frac{1}{2}\int_k^\infty \frac{s_{k'}}{k'}\,\mathrm{d}k' \int_0^k \int_0^k T_{mag}^{(i)}(k',p,q)\,\mathrm{d}p\,\mathrm{d}q \\ & -\frac{1}{2}\int_0^k \frac{s_{k'}}{k'}\,\mathrm{d}k' \int_k^\infty \int_k^\infty T_{mag}^{(i)}(k',p,q)\,\mathrm{d}p\,\mathrm{d}q.\end{aligned} \tag{7.20}$$

Following the approach explained in § 7.1 the integral becomes independent of k and one obtains the following expression for the flux of magnetic helicity through k

$$\begin{aligned}\Pi_H(k) \;=\; & k^{2-\beta'} \int_0^1 \mathrm{d}v \int_1^{1+v} \frac{\mathrm{d}w}{w} \\ & \times \left(s_w T_{mag}^{(i)}(w,1,v) \left[\frac{w^{\beta'-2}-1}{\beta'-2}\right] + s_v T_{mag}^{(i)}(v,1,w) \left[\frac{v^{\beta'-2}-1}{\beta'-2}\right]\right).\end{aligned} \tag{7.21}$$

7.3. *Cascades and wavenumber-dependent transfers of total energy and magnetic helicity*

From the expressions (7.17) and (7.21) for the fluxes of total energy and magnetic helicity, respectively, it is now possible to determine the sign of the fluxes and hence the direction of energy and magnetic helicity transfers using the results from the stability analysis. If the total energy flux is positive, energy is transferred from smaller to larger wavenumbers and if it is negative, energy is transferred from larger

to smaller wavenumbers. As the magnetic helicity is not positive definite, the situation is slightly different. For positive magnetic helicity a positive flux indicates forward transfer just as for the total energy. For negative magnetic helicity a negative flux indicates forward transfer while a positive flux indicates inverse transfer. However, as this situation is symmetric we assume positive helicity throughout the analysis.

In § 6 unstable solutions of (3.3) and (3.4) were interpreted as leading to energy transfer out of the unstable mode into the two modes it interacts with for a given helical mode interaction (i). If U_{s_p} and B_{s_p} are the unstable modes, this interpretation leads to

$$\partial_t |B_{s_p}|^2 = T^{(i)}_{mag}(p, k, q) < 0, \tag{7.22}$$

and

$$\partial_t |U_{s_p}|^2 = T^{(i)}_{HD}(p, k, q) + T^{(i)}_{LF}(p, k, q) < 0. \tag{7.23}$$

The instability assumption therefore attributes signs to the transfer terms, which will determine their respective contributions to the overall energy (and magnetic helicity) transfer. Note that $\partial_t |U_{s_p}|^2$ and $\partial_t |B_{s_p}|^2$ cannot have different signs, as both signs are determined from the existence of exponentially growing solutions of the system (4.6).

We now treat the three helicity combinations which lead to unstable solutions separately assuming without loss of generality that $s_p = 1$. Having determined the signs of the transfer terms within our framework, we now use these results to calculate the contributions of the individual transfer terms to the fluxes of total energy and magnetic helicity though a given wavenumber.

7.3.1. *Total energy cascades*

For the (inertial range) energy cascade the flux is wavenumber independent leading to $\beta = 3$ in (7.17). Hence the integrand in (7.17), which determines the sign of the total energy flux, becomes

$$I_E = T^{(i)}(w, 1, v) \ln w + T^{(i)}(v, 1, w) \ln v, \tag{7.24}$$

where we remind the reader of the wavenumber ordering $v \leqslant 1 \leqslant w$. That is, the term $T^{(i)}(w, 1, v)$ describes energy transfer in and out of the largest wavenumber modes while $T^{(i)}(v, 1, w)$ describes energy transfer in and out of the smallest wavenumber modes.

Using the signs of the transfer terms determined for the different helicity combinations depending on wavenumber ordering, we can now deduce which helicity combinations contribute to forward or inverse cascades of total energy.

(1) $s_v = s_1 = s_w$

For this case we can deduce from the results of the stability analysis summarised in tables 1–3 that $T^{(i)}(1, v, w) < 0$, as modes corresponding to the middle wavenumber are unstable, while $T^{(i)}(v, 1, w) > 0$, as modes corresponding to the smallest wavenumber are stable and hence these modes can only receive energy from the modes at higher wavenumbers. The sign of $T^{(i)}(w, 1, v)$ depends on the values of cross-helicity and the ratio of magnetic to kinetic energy. For a magnetically dominated system $T^{(i)}(w, 1, v) < 0$ and we obtain in this case an inverse cascade of total energy, as

$$I_E = T^{(i)}(w, 1, v) \ln w + T^{(i)}(v, 1, w) \ln v < 0. \tag{7.25}$$

If the kinetic energy is much larger than the magnetic energy, cancellations between the two terms in I_E occur. The term $T^{(i)}(w, 1, v) \ln w$ is now positive, since the modes

at the largest wavenumber can only receive energy, thus contributing to a forward cascade. For intermediate cases the value of the cross-helicity becomes decisive as high cross-helicity quenches the inverse transfer in this case. In summary, we expect inverse cascade contributions from this combination of helicities if the magnetic energy dominates, while for larger kinetic energy high values of cross-helicity quench the inverse transfer contribution to some extent.

(2) $s_v \neq s_1 = s_w$

From tables 1–3 the instability assumption imposes $T^{(i)}(w, 1, v) < 0$ and $T^{(i)}(v, 1, w) > 0$ as modes corresponding to the largest wavenumbers are unstable, while modes corresponding to the smallest wavenumber are stable. This implies

$$I_E = T^{(i)}(w, 1, v) \ln w + T^{(i)}(v, 1, w) \ln v < 0, \tag{7.26}$$

thus we conclude that this combination of helicities leads to an inverse energy cascade as $I_E < 0$, and we note that this case behaves differently to its hydrodynamic analogue, where it led to an inverse cascade of kinetic energy (Waleffe 1992) for non-local interactions and a direct cascade for local interactions. We also note that this inverse cascade should always be present, as it is not subject to constraints from $H_c(p)$ and $|U_{s_p}|/|B_{s_p}|$.

(3) $s_v = s_1 \neq s_w$

Analogously, we obtain $T^{(i)}(1, v, w) < 0$ and $T^{(i)}(w, 1, v) > 0$, since the modes corresponding to the middle wavenumber are unstable while modes corresponding to the largest wavenumber are stable. As the stability of the remaining transfer term $T^{(i)}(v, 1, w)$ depends on several constraints, no clear assessment is possible. If we assume the lowest wavenumber modes to be unstable, that is $T^{(i)}(v, 1, w) < 0$, we obtain a contribution towards a direct cascade. However, if we assume them to be stable, contributions to inverse and direct cascades are possible. We note that the instability leading to forward transfer in this case is damped by high values of $H_c(p)$.

(4) $s_1 \neq s_w = s_v$

In this case we obtain $T^{(i)}(1, v, w) > 0$ and $T^{(i)}(w, 1, v) < 0$, since the modes corresponding to the middle wavenumber are stable while modes corresponding to the largest wavenumber are unstable. Again the sign of the remaining transfer term $T^{(i)}(v, 1, w)$ depends on several constraints. If we assume the lowest wavenumber modes to be stable, that is $T^{(i)}(v, 1, w) > 0$, we obtain a contribution towards an inverse cascade. However, if we assume them to be unstable, contributions to inverse and direct cascades are possible. We note that the instability leading to inverse transfer in this case is damped by high values of $H_c(p)$.

7.3.2. *Magnetic helicity transfer in the inertial range of total energy*

For $\beta' = 3$, the integrand I_H in (7.21) becomes

$$I_H = T^{(i)}_{mag}(w, 1, v) s_w (w - 1) + T^{(i)}_{mag}(v, 1, w) s_v (v - 1). \tag{7.27}$$

Using the signs of the transfer terms determined for the three helicity combinations, we can now deduce which helicity combinations contribute to a forward or inverse cascade of magnetic helicity. As can be seen in (7.27), there is an explicit dependence of the magnetic helicity flux on the helicities of the interacting modes. In the following we assume $s_1 = 1$.

(1) $s_v = s_1 = s_w$

The integrand I_H becomes

$$I_H = T^{(i)}_{mag}(w, 1, v)(w - 1) + T^{(i)}_{mag}(v, 1, w)(v - 1). \tag{7.28}$$

As the signs of the magnetic energy transfer term deduced from the stability analysis are the same as for the total energy and $\ln w$ and $w-1$ are both positive while $\ln v$ and $v-1$ are both negative, the result for the helicity transfer reflects the results for the total energy cascade. Thus, for this helicity combination, total energy and magnetic helicity will be transferred in the same direction, which can be both forward and inverse in this case.

(2) $s_v \neq s_1 = s_w$

The integrand I_H becomes

$$I_H = T^{(i)}_{mag}(w, 1, v)(w-1) - T^{(i)}_{mag}(v, 1, w)(v-1), \tag{7.29}$$

where the contributions from the smallest wavenumber modes now enter with the opposite sign. Compared to the total energy flux, which was purely inverse in this case, we obtain the possibility of simultaneously a forward helicity flux and an inverse energy flux.

(3) $s_v = s_1 \neq s_w$

The integrand I_H becomes

$$I_H = -T^{(i)}_{mag}(w, 1, v)(w-1) + T^{(i)}_{mag}(v, 1, w)(v-1), \tag{7.30}$$

where the contributions from the largest wavenumber modes now enter with the opposite sign. Compared to the total energy cascade, again we find that it is possible to have a transfer of magnetic helicity in the opposite direction to the transfer of total energy.

(4) $s_1 \neq s_w = s_v$

The integrand I_H becomes

$$I_H = -T^{(i)}_{mag}(w, 1, v)(w-1) - T^{(i)}_{mag}(v, 1, w)(v-1), \tag{7.31}$$

where the contributions from both transfer terms now enter with the opposite sign. That is, magnetic helicity and total energy are transferred in opposite directions.

In this subsection we determined the direction of the magnetic helicity transfer in the inertial range of total energy for different combinations of helicities and compared the results to those for the total energy cascade. We found that a cascade of total energy is possible in one direction while the transfer of magnetic helicity may proceed in the opposite direction.

7.3.3. *Magnetic helicity cascades*

In the inertial range of magnetic helicity the flux of magnetic helicity is wavenumber independent resulting in $\beta' = 2$ in (7.21). Therefore the integrand I_H in (7.21) becomes

$$I_H = T^{(i)}_{mag}(w, 1, v)s_w \ln w + T^{(i)}_{mag}(v, 1, w)s_v \ln v. \tag{7.32}$$

For the different helicity combinations this leads to

(1) $s_v = s_1 = s_w$

The integrand in this case is of the same form as the integrand I_E for the total energy cascade (that is, if $\beta = 3$ in I_E)

$$I_H = T^{(i)}_{mag}(w, 1, v) \ln w + T^{(i)}_{mag}(v, 1, w) \ln v, \tag{7.33}$$

hence the results for the cascades of magnetic helicity are the same as for the cascades of total energy.

(2) $s_v \neq s_1 = s_w$

The integrand in this case has a different form compared to the integrand I_E for the total energy

$$I_H = T^{(i)}_{mag}(w, 1, v) \ln w - T^{(i)}_{mag}(v, 1, w) \ln v, \tag{7.34}$$

hence the results for the cascades of magnetic helicity are different from the total energy cascades. In particular, this case may lead to a non-helical reverse energy transfer while the helicity cascade may be forwards, due to the contribution from $T^{(i)}_{mag}(v, 1, w)$ now having the opposite sign in I_H compared to I_E.

(3) $s_v = s_1 \neq s_w$

Again, the integrand in this case has a different form compared to the integrand I_E for the total energy

$$I_H = -T^{(i)}_{mag}(w, 1, v) \ln w + T^{(i)}_{mag}(v, 1, w) \ln v, \tag{7.35}$$

hence the results for the cascades of magnetic helicity differ from the total energy cascades. In particular, this case may lead to a forward energy transfer while the helicity cascade may be backwards, due to the contribution from $T^{(i)}_{mag}(w, 1, v)$ now having the opposite sign in I_H compared to I_E.

(4) $s_1 \neq s_w = s_v$

Now I_H and I_E have opposite signs

$$I_H = -T^{(i)}_{mag}(w, 1, v) \ln w - T^{(i)}_{mag}(v, 1, w) \ln v = -I_E, \tag{7.36}$$

hence this case leads to helicity transfer and energy transfer in opposite directions.

7.3.4. *Magnetic energy transfer in the inertial range of magnetic helicity*

For $\beta' = 2$, the contributions to the integrand I_E due to magnetic energy transfer are

$$I_{E_{mag}} = -T^{(i)}_{mag}(w, 1, v) \left(\frac{1}{w} - 1\right) - T^{(i)}_{mag}(v, 1, w) \left(\frac{1}{v} - 1\right). \tag{7.37}$$

The signs of T_{mag} and T are the same by (7.22)–(7.23), and $\ln w$ and $w - 1$ are both positive while $\ln v$ and $v - 1$ are both negative. Hence, the result for the contributions of these terms to the total energy transfer in the inertial range of magnetic helicity is the same as in the inertial range of total energy for all helicity combinations. That is, magnetic energy transfer and conversion in the inertial ranges of total energy and magnetic helicity proceed in the same direction.

This assessment of contributions to forward and inverse transfers and cascades is based on an analysis of the nonlinear terms in the MHD equations only, thus neglecting the symmetry-breaking effect of dissipation creating an energy sink at the small scales. Accounting for this effect, it is plausible that the contributions from transfer terms leading to forward transfer are higher weighted than contributions leading to inverse transfer. This is particularly relevant in interactions where forwards and reverse contributions are present and the overall transfer depends on cancellations between the two terms. It would perhaps be safest to attribute these cases to forwards rather than inverse energy cascades.

Although it is not possible to exactly determine which helical interactions are higher weighted than others, some information can be obtained from the magnitude of the geometric factor g_{kpq} defined in (3.5). The magnitude of g_{kpq} depends on the

helicity combinations since it involves the helicity-dependent factor $I = s_k k + s_p p + s_q q$. Therefore it parametrises the strength of a given helical interaction, and the case of all helicities being of the same sign gives the largest value of $|I|$, since in this case $|I| = |k + p + q|$.

For the reverse transfers, that is, for $k < p, q$, the factor $|I|$ takes the smallest value for the case $s_k = s_p \neq s_q$, since $|I| = |k + (p - q)|$. Note that in this case I becomes small for small k even in the non-local limit $k \ll p \simeq q$, suggesting that the non-helical reverse transfer found in this case is less efficient in increasing spectral power at the very low wavenumbers. The remaining class of helical interactions $s_k \neq s_p = s_q$ leads to $|I| = |k - (p + q)|$. In this case $|I|$ does not necessarily become small for small k which is due to the contribution of non-local interactions, where p and q are large compared to k. According to the results from the stability analysis, in the non-local limit unstable solutions occur for the case $s_k = s_p = s_q$ only if $|B_{s_p}| > |U_{s_p}|$ and for the case $s_k \neq s_p = s_q$ if $|U_{s_p}| > |B_{s_p}|$.

It is therefore possible to deduce within the framework of the instability assumption that most of the increase in energy at the very largest scales (in a magnetically dominated system) is mainly due to a breaking of mirror symmetry, which had been established before by Frisch *et al.* (1975) using a different approach. That is, it is due to the presence of kinetic and magnetic helicity, since interactions of the type $s_k = s_p = s_q$, which account for most of the inverse transfer, can only occur in significant numbers for fields consisting of many modes with the same helicity. Recent numerical results in hydrodynamics showed that there is an overall reverse flux of energy only when the system mainly contains helical modes of the same sign. As soon as a small amount of oppositely polarised modes is introduced, the usual direct cascade is recovered (Sahoo, Bonaccorso & Biferale 2015).

In summary, in this section we determined the direction of total energy and magnetic helicity transfers in their respective inertial ranges. Not surprisingly, we found that fully helical magnetic fields lead to inverse cascades of magnetic helicity and inverse transfer of magnetic energy, but the analysis also showed that an inverse energy cascade is possible for non-helical magnetic fields, which is a new theoretical result. However, due to the coupling of the momentum and induction equations, within this framework it is not possible to determine the nature of the energy transfers resulting from an instability of a given steady solution, since the same eigenvalue controls the growth of the exponential solution of (4.6) for both the magnetic and the velocity field. Nevertheless, for some special cases the evolution equations (3.3)–(3.4) decouple and more detailed information becomes available. These cases are treated in the following section.

8. Special solutions and the (kinematic) dynamo

Having established the general case, we now draw attention to special cases where the analysis becomes much simpler and which are relevant to specific problems in MHD such as the kinematic dynamo. In § 4.2 we analysed the stability of general steady solutions of the dynamical system (3.3)–(3.4), which describes the evolution of a triad of interacting helical modes. Using the notation (4.1), the general steady solutions were of the form $(0, U_{s_p}, 0; 0, B_{s_p}, 0)$. In this section we now study the cases where either $U_{s_p} = 0$ or $B_{s_p} = 0$, that is we analyse the stability of steady solutions of (3.3)–(3.4) of the form $(0, U_{s_p}, 0; 0, 0, 0)$ and $(0, 0, 0; 0, B_{s_p}, 0)$. The former case may be of particular interest due to its relation to dynamo action.

8.1. *The kinematic dynamo*

For small magnetic fields the Lorentz force is small compared to inertial forces, and can be neglected in the momentum equation. This decouples the momentum equation from the induction equation and defines the kinematic dynamo problem. In our setting, it corresponds to $|U_{s_p}|/|B_{s_p}| \gg 1$, and terms proportional to $|B_{s_p}|$ can be neglected as they are very small compared to terms proportional to $|U_{s_p}|$.

Alternatively, one could also consider the steady solution $B_{s_p} = 0$ while $U_{s_p} \neq 0$. This would correspond to a stability analysis of a flow field at a particular length scale subject to small perturbations of the magnetic and velocity fields, where the magnetic field perturbation may be viewed as the magnetic seed field to be amplified by dynamo action. In this setting we observe from (3.3) that the term corresponding to the Lorentz force disappears while in (4.5) terms involving B_{s_p} disappear, thus the system simplifies to

$$\partial_t^2 u_{s_k} = |g_{kpq}|^2 (s_p p - s_q q)(s_k k - s_p p)\, |U_{s_p}|^2 u_{s_k}, \tag{8.1}$$

$$\partial_t^2 b_{s_k} = -|g_{kpq}|^2 s_k k\, s_q q\, |U_{s_p}|^2 b_{s_k}. \tag{8.2}$$

As the only contribution to the evolution of the magnetic field now comes from the velocity field, we associate the remaining terms in (3.4) with dynamo action. From (8.2) we observe that this system has exponential solutions leading to magnetic field growth if $s_k \neq s_q$, regardless of wavenumber ordering. So for energy transfer from U_{s_p} into b_{s_k} (and b_{s_q}) to become possible, the magnetic modes at wavenumbers k and q should be of opposite helicity.

For small k, non-local interactions with $k \ll p \simeq q$ provide most transfer into b_{s_k}. This is because the eigenvalue determining the growth of the exponential solution of (8.2) is larger for $q \gg k$ than for $q \simeq k$, thus the perturbations should grow faster in the former than in the latter case. Hence, according to the instability assumption, U_{s_p} loses energy in favour of b_{s_k} mainly due to non-local interactions if b_{s_k} describes the largest scales of the system.

8.1.1. *The α-effect*

One well-known example of a large-scale dynamo is the α-effect of mean-field electrodynamics (see e.g. Moffatt 1978), where α is a coefficient in the mean-field induction equation related to the kinetic helicity of the flow. The α-effect leads to a generation of large and small-scale magnetic helicities of opposite sign (Brandenburg 2001, 2003). It is a mean-field description of the stretch-twist-fold (STF) dynamo (Vainshtein & Zeldovich 1972; Childress & Gilbert 1995; Mininni 2011), which describes how a positively helical velocity field generates magnetic field perturbations leading to the large-scale component of the magnetic field becoming negatively helical. By conservation of magnetic helicity, the small-scale component of the magnetic field then has to become positively helical (and more so if the initial magnetic field was positively helical). That is, the small-scale magnetic and kinetic helicities are of the same sign.

It is plausible that the type of interaction $(0, U_{s_p}, 0; 0, B_{s_p} = 0, 0)$ for $k < p, q$ with $s_k \neq s_p = s_q$ can be associated with an STF dynamo and hence the α-effect. First, non-zero small-scale kinetic helicity (we have $s_p = s_q$) is present. Second, the magnetic field growth at the large scales is described by (8.2), where magnetic fluctuations at k and q of opposite helicities are necessary to obtain an unstable solution. That is, the large-scale magnetic field has opposite helicity to the small scale one, reminiscent of the α-dynamo. We also note that this combination of helicities produces a transfer of

kinetic energy from small to large scales (Waleffe 1992). Thus this type of interaction feeds into the magnetic and velocity fields on scales larger than the characteristic scale $L = 1/p$ of the velocity field. The magnetic field mode which is amplified by this process has helicity opposite to the velocity field at p, which conforms to expectations in terms of STF dynamo action and the α-effect.

8.2. *Excitation of a flow by the Lorentz force*

For the other special solution $(0, 0, 0; 0, B_{s_p} \neq 0, 0)$ the system (4.4)–(4.5) simplifies to

$$\partial_t^2 u_{s_k} = |g_{kpq}|^2 (s_p p - s_q q) s_q q \, |B_{s_p}|^2 u_{s_k}, \tag{8.3}$$

$$\partial_t^2 b_{s_k} = -|g_{kpq}|^2 s_k k (s_k k - s_p p) \, |B_{s_p}|^2 b_{s_k}, \tag{8.4}$$

and we note that the inertial term in (3.3) and the 'dynamo' term in (3.4) are now absent and the system of coupled ODEs has split into two decoupled ODEs. This case may perhaps be associated with the generation of turbulence caused by the action of the Lorentz force on the fluid (i.e. energy conversion from B_{s_p} to u_{s_k} or u_{s_q}) and interscale transfer of magnetic energy from B_{s_p} into b_{s_k} or b_{s_q}. Exponentially growing solutions of (8.4) only occur if $s_p = s_k$ and $k < p$, leading to a reverse transfer of magnetic energy. Exponentially growing solutions of (8.3) occur for $p > q$ and $s_p = s_q$ leading to forward and reverse transfers corresponding to $k > p$ and $k < p$, respectively. Interestingly, energy transfer only becomes possible if the magnetic field is helical and the helicity of the velocity field mode does not affect the analysis.

9. Conclusions

The four main results of the present work are: First, unlike in non-conducting fluids (Waleffe 1992), the stability analysis shows that in MHD turbulence energy can be transferred away from the smallest scales in a triad interaction. Second, the stability analysis reveals mechanisms for reverse energy transfer for non-helical magnetic fields, in which case it does not need to be driven by the inverse transfer of magnetic helicity. Third, forward energy transfers are more quenched in regions of high cross-helicity than reverse energy transfers. Fourth, we expect significant cancellations to occur between the contributions to forward and reverse transfers, as on several occasions they occur with opposite signs in the same equation. Our theoretical analysis was conducted within the framework of the instability assumption, and it is crucial to discuss the results within the wider context of MHD turbulence research.

Interscale energy transfers between the two different vector fields as well as within the same fields have been studied by several groups for freely decaying (Debliquy *et al.* 2005; Brandenburg *et al.* 2015) and stationary (Brandenburg 2001; Alexakis *et al.* 2005; Carati *et al.* 2006; Cho 2010) MHD turbulence as well as for the kinematic dynamo regime (Mininni, Alexakis & Pouquet 2005) and for magnetic helicity transfer (Alexakis *et al.* 2006), using shell-filtered transfer terms calculated from DNS or from a helical shell model (Stepanov *et al.* 2015). In the stationary case, it was found that transfers between the same fields are mainly local while transfers between different fields were non-local, and transfers from the injection scale to the largest scales in the system were observed. In the decaying case, energy transfers were generally found to be mainly local. However, transfers

between different fields were more non-local than transfers between the same fields. Furthermore, large cancellations occurred between the contributions to forward and reverse transfers (Debliquy *et al.* 2005). The analysis presented here also predicts cancellations between these contributions to occur, thus being consistent with the aforementioned numerical results.

In terms of locality and non-locality of energy (and helicity) transfer, we found that non-local interactions contribute to forward transfer only for interactions of helical modes with unlike helicity and mainly if the kinetic energy exceeds the magnetic energy. Interestingly, for inverse transfers we find less constraints on non-local interactions. In particular for magnetically dominated systems non-local interactions between modes of like helicity contribute to reverse energy transfer. In view of the cancellations that occur between forward and reverse transfers, the inverse cascade may thus have a significant non-local component which is not cancelled by forward transfers within the same triad interaction.

A numerical study of large-scale magnetic field generation in helically forced globally isotropic MHD turbulence was carried out by Brandenburg (2001). It was found that the injection of energy from the velocity field into the magnetic field occurs directly from the forcing scale into the largest resolved scale, implying that this is a non-local process. Due to the non-locality of the observed increase in spectral power of the magnetic field at the lowest resolved wavenumber $k = 1$ and the excellent agreement of numerical results with an α-dynamo model, the transfer of energy into the $k = 1$ mode is explained by the α-effect rather than an inverse cascade, and it is shown to occur after saturation of the small-scale dynamo. Our results in § 8 suggest that one type of helical mode interaction may be mapped to the α-effect, and we established that large-scale dynamo action is more active in the non-local limit than certain other types of interactions.

One of the main results of the present work is the possibility of inverse energy transfer for non-helical magnetic fields. Such inverse transfer has recently been found in high resolution DNS of slightly compressible (Brandenburg *et al.* 2015) and relativistic (Zrake 2014) MHD turbulence. An analysis of interscale transfers showed that this inverse transfer was mainly due to energy transfer away from the medium scale (see supplemental material of Brandenburg *et al.* (2015), last figure), while energy transfer away from the smallest scales also occurred. The analytic approach put forward in the present paper also shows that energy is transferred away from the medium and small scales for interactions of modes with unlike helicities, thus being qualitatively consistent with these numerical results. However, since no numerical work decomposing the MHD equations into helical contributions as suggested by Biferale *et al.* (2012) and Biferale & Titi (2013) has been carried out so far, we are not in a position to claim numerical confirmation of our results.

Having discussed numerical results, we now turn to measurements of energy transfer in the solar wind. Unlike in our own analysis and in the numerical results discussed so far except for (Cho 2010), a background magnetic field is present in the solar wind. Recent measurements at 1 AU (Stawarz *et al.* 2010) showed negative Elsässer fluxes in regions of high cross-helicity, giving possible evidence of inverse energy transfer in these regions, which cannot be explained by selective decay as cross-helicity cascades forwards (Frisch *et al.* 1975). Our results may be helpful in explaining this phenomenon as one of the results we obtained was a quenching of forward energy transfer in regions of high cross-helicity, leaving more inverse transfer to perhaps dominate the dynamics in these regions.

In subsequent work (Coburn *et al.* 2014) concerns were raised on the implications of the effect of expansion in the solar wind especially in regions of high H_c.

Expansion effects had been neglected in the previous analysis. The authors restrict their measurements to regions where the relative cross helicity σ_c is not too large, that is $0 \leqslant |\sigma_c| \leqslant 0.5$ and measure positive energy fluxes on average, while the instantaneous flux shows large variations including negative values. It is shown that the broad distribution of the measured instantaneous fluxes is related to intermittency of the energy cascade in terms of the variability of the energy flux (Politano & Pouquet 1995; Karimabadi *et al.* 2013), and not caused by experimental uncertainty. The various possibilities of energy transfer in forward and reverse directions determined in the present work are consistent with these measurements, as they also would result in broader tails of the probability distribution of the energy flux, even if on average energy transfer proceeds in the forward direction. As for the concerns about the validity of the negative fluxes measured by Stawarz *et al.* (2010), our results do suggest that the measured inverse fluxes may be a genuine effect due to quenching of forward energy transfers if H_c is large.

Since most of this discussion is based on statements of plausibility rather than certainty, more work clearly has to be carried out before a decisive result on energy transfer in MHD turbulence can be achieved, and we hope that our analysis constitutes a step forwards in this direction. As suggested by Biferale *et al.* (2012), Biferale & Titi (2013), one could study energy and helicity transfers numerically by projecting out helical modes of a particular sign, similar to work done by Biferale *et al.* (2012), Biferale & Titi (2013) and Sahoo *et al.* (2015) in hydrodynamic turbulence. However, numerical verification of reverse spectral transfer due to the particular non-helical interactions found in the present work may be difficult to obtain in that framework, and a particular DNS study concentrating on inverse transfer for non-helical magnetic fields using the full MHD equations subject to small-scale forcing may be needed in order to provide further insight. An analysis of Fourier-filtered transfer terms from DNS of highly unbalanced MHD turbulence compared to balanced MHD turbulence could be carried out in order to verify (or otherwise) the proposed quenching of forward transfers by high values of H_c, especially as it is not possible to quantify this effect from theoretical analysis only. On the analytical side, the present work may be extended to include the effects of a background magnetic field and of compressive fluctuations, which would be included in the decomposition of the velocity field as modes parallel to the wavevector $\boldsymbol{k}$. Asides from providing an advance in MHD turbulence research on a fundamental level, this work may contribute to the further theoretical understanding of various physical processes involving inverse cascade and dynamo action. This includes the evolution and origin of cosmological and galactic magnetic fields as well as solar physics and the dynamics of laboratory plasmas and turbulence in liquid metal flows.

Acknowledgements

A.B. acknowledges support from the UK Science and Technology Facilities Council, M.L. and M.M. are funded by the UK Engineering and Physical Sciences Research Council (EP/K503034/1 and EP/M506515/1) and J.J. was supported by a University of Edinburgh Physics and Astronomy Summer Student Scheme Fellowship.

Appendix A. The dependence of Q on the cross-helicity

In § 4, the parameter Q was defined as $Q = \alpha\delta - \beta\gamma$, where α, β, γ and δ were the entries of the matrix in (4.6). Using the expressions for these terms given in (4.10),

we obtain

$$Q = |g_{kpq}|^4 s_k k s_q q (s_k k - s_p p)(s_q q - s_p p) \left(|U_{s_p}|^4 + |B_{s_p}|^4 - 2\,\mathrm{Re}([U^*_{s_p} B_{s_p}]^2) \right). \tag{A 1}$$

However, in (4.14), instead of the term $\mathrm{Re}([U^*_{s_p} B_{s_p}]^2)$ a term involving $H_c(p)$ appeared.

In general, the helical coefficients U_{s_p} and B_{s_p} are related by a complex number $M = m + \mathrm{i}n$ such that $B_{s_p} = M U_{s_p}$. Expressions for m and n can be found by decomposing the two fields into their real and imaginary parts. Let $U_{s_p} = U_1 + \mathrm{i}U_2$ and $B_{s_p} = B_1 + \mathrm{i}B_2$. Then

$$m = \frac{1}{|U_{s_p}|^2}(U_1 B_1 + U_2 B_2) \quad \text{and} \tag{A 2}$$

$$n = \frac{1}{|U_{s_p}|^2}(U_1 B_2 - U_2 B_1), \tag{A 3}$$

and we note the constraint $n^2 = |B_{s_p}|^2/|U_{s_p}|^2 - m^2$ which follows from the definition of M. Decomposing the cross-helicity in the same way results in $H_c(p) = |U_{s_p}|^2 m$. Now we can relate $\mathrm{Re}([U^*_{s_p} B_{s_p}]^2)$ to the cross-helicity by rewriting it in terms of the components of U_{s_p} and B_{s_p}:

$$\mathrm{Re}([U^*_{s_p} B_{s_p}]^2) = (U_1 B_1 + U_2 B_2)^2 - (U_1 B_2 - U_2 B_1)^2 \tag{A 4}$$

$$= |U_{s_p}|^4 m^2 - |U_{s_p}|^4 \left(\frac{|B_{s_p}|^2}{|U_{s_p}|^2} - m^2 \right) \tag{A 5}$$

$$= 2H_c(p)^2 - |U_{s_p}|^2 |B_{s_p}|^2, \tag{A 6}$$

and we obtain (4.14) by substitution of this expression for $\mathrm{Re}([U^*_{s_p} B_{s_p}]^2)$ into (A 1).

Since the maximum and minimum values of $|H_c(p)|$ are $|U_{s_p}||B_{s_p}|$ and 0 respectively, it is useful to define the relative cross-helicity $\rho = H_c(p)/(|U_{s_p}||B_{s_p}|)$, which takes values between -1 and 1. We obtain

$$\mathrm{Re}([U^*_{s_p} B_{s_p}]^2) = |U_{s_p}|^2 |B_{s_p}|^2 (2\rho^2 - 1), \tag{A 7}$$

which is bounded by $-|U_{s_p}|^2|B_{s_p}|^2$ and $|U_{s_p}|^2|B_{s_p}|^2$, where the first value is the case of vanishing cross-helicity and the latter occurs when there is maximal cross-helicity. This implies that the term $(|U_{s_p}|^4 + |B_{s_p}|^4 + 2|U_{s_p}|^2|B_{s_p}|^2 - 4H_c(p)^2)$ in (4.14) cannot be negative.

Appendix B. $x^2 - Q > 0$ for specific cases

In § 5.1, the result was dependent on whether $x^2 - Q$ is positive or negative. Recall that the helicity combinations in question were $s_k = s_q \neq s_p$ and $s_k = s_p = s_q$ with the wavenumber ordering $p \leqslant k, q$ for the latter case. Therefore $x^2 - Q$ becomes

$$\begin{aligned} x^2 - Q = \tfrac{1}{4} \big[& |U_{s_p}|^4 (kq + (k \pm p)(q \pm p))^2 + |B_{s_p}|^4 (k(k \pm p) + q(q \pm p))^2 \\ & + 2|U_{s_p}|^2 |B_{s_p}|^2 [kq + (k \pm p)(q \pm p)][k(k \pm p) + q(q \pm p)] \big] \\ & - [kq(k \pm p)(q \pm p)](|U_{s_p}|^4 + |B_{s_p}|^4 - 2\mathrm{Re}([U^*_{s_p} B_{s_p}]^2)) \end{aligned}$$

$$= \tfrac{1}{4}\left[|U_{s_p}|^4(kq-(k\pm p)(q\pm p))^2+|B_{s_p}|^4(k(k\pm p)-q(q\pm p))^2\right.$$
$$\left.+2|U_{s_p}|^2|B_{s_p}|^2[kq+(k\pm p)(q\pm p)][k(k\pm p)+q(q\pm p)]\right]$$
$$+2\mathrm{Re}([U^*_{s_p}B_{s_p}]^2)[kq(p\pm p)(q\pm p)]. \tag{B 1}$$

In general, we have $|\mathrm{Re}([U^*_{s_p}B_{s_p}]^2)| \leqslant |U_{s_p}|^2|B_{s_p}|^2$ (see appendix A), hence assume $\mathrm{Re}([U^*_{s_p}B_{s_p}]^2) = -|U_{s_p}|^2|B_{s_p}|^2$ as this would be the most negative value this term can take. It corresponds to zero cross-helicity at $\boldsymbol{p}$. Equation (B 1) is now an inequality and reads

$$x^2-Q \geqslant \tfrac{1}{4}\left[|U_{s_p}|^4(kq-(k\pm p)(q\pm p))^2+|B_{s_p}|^4(k(k\pm p)-q(q\pm p))^2\right]$$
$$+\tfrac{1}{2}|U_{s_p}|^2|B_{s_p}|^2[kq+(k\pm p)(q\pm p)][k(k\pm p)+q(q\pm p)]$$
$$-2|U_{s_p}|^2|B_{s_p}|^2[kq(k\pm p)(q\pm p)], \tag{B 2}$$

hence the result $x^2-Q>0$ follows immediately if we can show

$$[kq+(k\pm p)(q\pm p)][k(k\pm p)+q(q\pm p)]-4kq(k\pm p)(q\pm p)\geqslant 0. \tag{B 3}$$

For this purpose, set $a^\pm \equiv (k\pm p)$ and $b^\pm \equiv (q\pm p)$. The expression on the left-hand side of (B 3) can now be further simplified

$$\begin{aligned}[kq+a^\pm b^\pm][ka^\pm+qb^\pm]-4kqa^\pm b^\pm &= k^2qa^\pm+(a^\pm)^2kb^\pm+q^2kb^\pm+(b^\pm)^2qa-4kqab\\ &= qa^\pm(k-b^\pm)^2+kb^\pm(q-a^\pm)^2\geqslant 0.\end{aligned} \tag{B 4}$$

The last line follows for the case $s_k=s_q\neq s_p$ since both $a^+\geqslant 0$ and $b^+\geqslant 0$, while for the case $s_k=s_p=s_q$ both $a^-\geqslant 0$ and $b^-\geqslant 0$ due to the wavenumber ordering $p\leqslant k,q$. Hence the inequality (B 3) is satisfied and $x^2-Q\geqslant 0$ in both cases.

Appendix C. Graphical determination of constraints on stability

As explained in the main body of the text, the term Q given in (4.14) determines the stability of the system (4.6) if $x<0$. As such, a solution is unstable if $Q<0$ or if $x^2-Q<0$, where the latter case is the more difficult to determine, as the sign of x^2-Q depends on the shape of the wavenumber triad, the cross-helicity and the ratio $|U_{s_p}|/|B_{s_p}|$. Given the multitude of possibilities that can emerge for this, the simplest way of determining the constraints on the stability of a solution of (4.6) is using a graphical method. For each combination of helicities we plot x^2–Q for several set values of $|U_{s_p}|/|B_{s_p}|$ and $H_c(p)$ in order to show in which parameter range instabilities are more likely to occur.

The dependence of x^2–Q on the triad k,p,q can be reduced to a dependence on the triad's shape by rescaling each wavenumber similar to the procedure in appendix B, which enables us to use two-dimensional plots and the triad geometry to obtain the necessary information. Figures 1–4 show the function $x^2(v,w)-Q(v,w)$ for the different cases shown in tables 1–3, where v and w correspond to the smallest and largest wavenumber in a given triad, rescaled by the middle one such that the triad geometry enforces the constraint $0<v\leqslant 1\leqslant w<1+v$, hence each wavenumber pair (v,w) describes a shape of triad. Each subfigure corresponds to set values of $H_c(p)$ and $|U_{s_p}|/|B_{s_p}|$, while each point (v,w) in a particular graph corresponds to a class of triad interactions characterised by their shape. Regions in wavenumber space

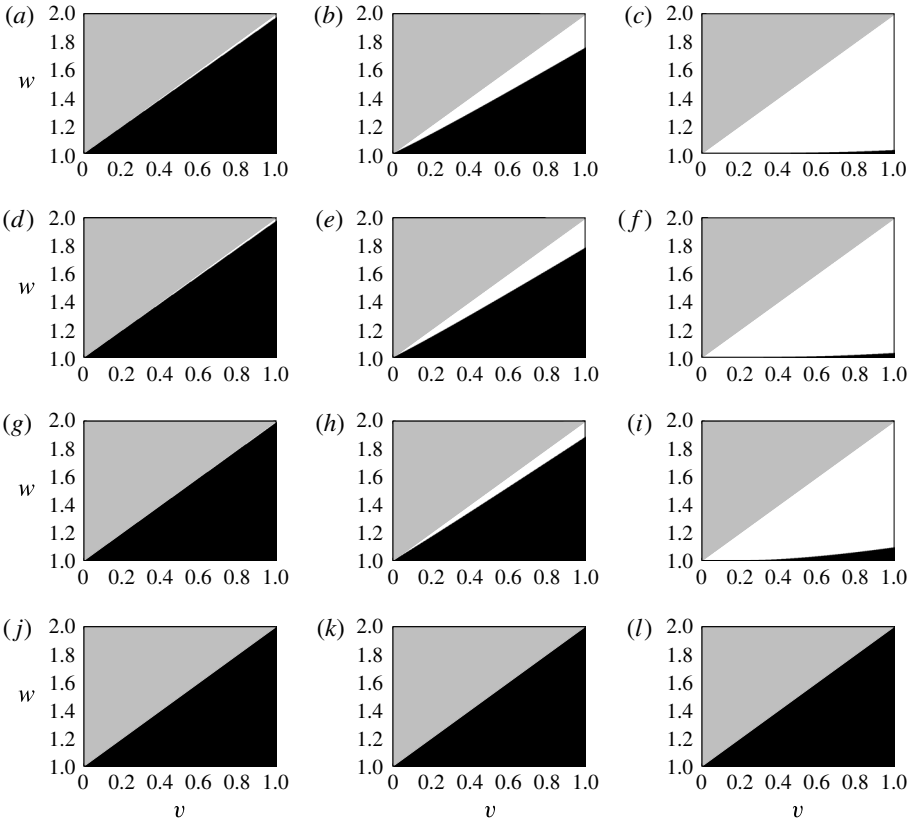

FIGURE 1. Plots of $f(v, w) = x^2 - Q$ for various values of $|U_{s_p}|/|B_{s_p}|$ and cross-helicity for case 1 in appendix C ($s_k \neq s_p = s_q$, $k < p < q$). The upper grey triangle is ruled out by the condition $w < 1 + v$ and unstable values are shown in white. The ratio $|U_{s_p}|/|B_{s_p}|$ increases from left to right, with each column of subfigures taking the values 0.01, 0.1 and 1 respectively, while each row takes the following values of relative cross-helicity: $H_c(p)/(|U_{s_p}||B_{s_p}|) = 0, 0.5, 0.9$ and 1.

excluded from the analysis by the constraints of the triad geometry are shaded in grey, positive values of $x^2 - Q$ leading to stability are indicated in black and negative values of $x^2 - Q$ leading to unstable solutions are marked white. Across the main four figures, $H_c(p)$ increases towards the bottom of the figure while $|U_{s_p}|/|B_{s_p}|$ increases from left to right, leading to the constraints summarised in tables 1–3. Depending on the wavenumber ordering, the definitions of v and w are slightly different, and we explain the procedures for each case individually.

(1) $s_k \neq s_p = s_q$ and $k < p < q$

In this case we rescale all wavenumbers by p, such that $v \equiv k/p$ and $w \equiv q/p$. As can be seen in figure 1, for decreasing $|U_{s_p}|/|B_{s_p}|$ and increasing $H_c(p)$ less and less unstable solutions occur and we obtain the constraints on split transfer shown in table 1.

(2) $s_k \neq s_p = s_q$ and $p < k < q$

In this case we rescale all wavenumbers by k, such that $v \equiv p/k$ and $w \equiv q/k$. As can be seen in figure 2, for decreasing $|U_{s_p}|/|B_{s_p}|$ and increasing $H_c(p)$ less and less

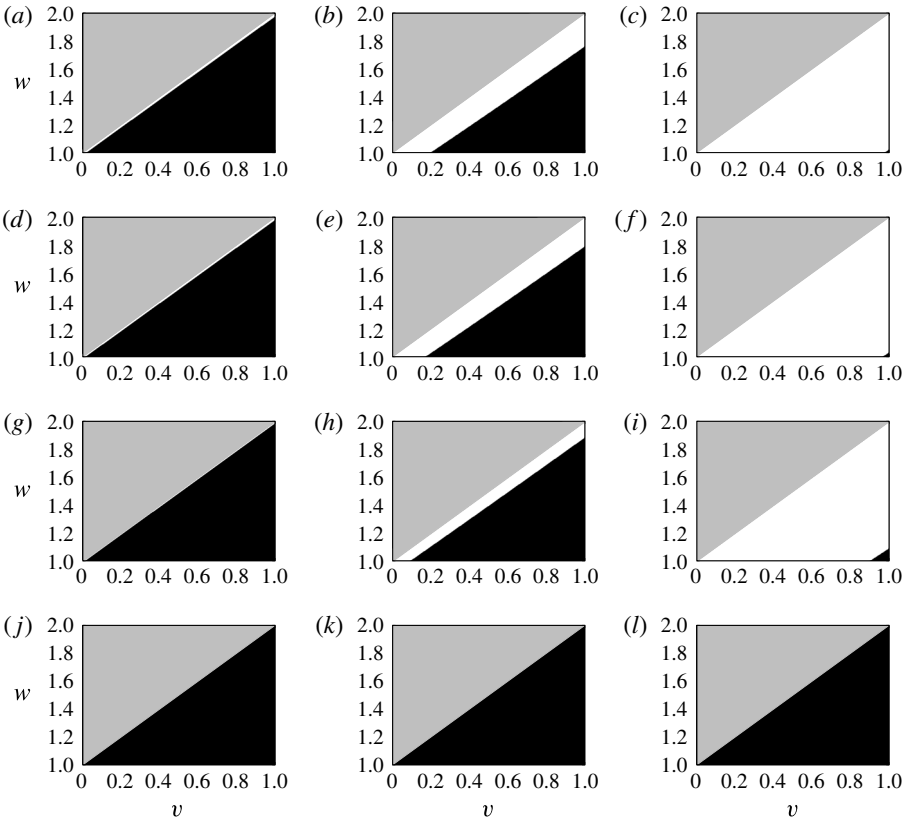

FIGURE 2. Plots of $f(v, w) = x^2 - Q$ for various values of $|U_{s_p}|/|B_{s_p}|$ and cross-helicity for case 2 in appendix C ($s_k \neq s_p = s_q$, $p < k < q$). The upper grey triangle is ruled out by the condition $w < 1 + v$ and unstable values are shown in white. The ratio $|U_{s_p}|/|B_{s_p}|$ increases from left to right, with each column of subfigures taking the values 0.01, 0.1 and 1 respectively, while each row takes the following values of relative cross-helicity: $H_c(p)/(|U_{s_p}||B_{s_p}|) = 0$, 0.5, 0.9 and 1.

unstable solutions occur and we obtain the constraints on forward transfer shown in table 3.

(3) $s_k = s_p \neq s_q$ and $p < k < q$

In this case we rescale all wavenumbers by k, such that $v \equiv p/k$ and $w \equiv q/k$. As can be seen in figure 3, for decreasing $|U_{s_p}|/|B_{s_p}|$ and increasing $H_c(p)$ less and less unstable solutions occur and we obtain the constraints on forward transfer shown in table 3.

(4) $s_k = s_p = s_q$ and $k < q < p$

In this case we rescale all wavenumbers by q, such that $v \equiv k/q$ and $w \equiv p/q$. As can be seen in figure 4, now for increasing $|U_{s_p}|/|B_{s_p}|$ and increasing $H_c(p)$ less and less triads lead to unstable solutions and we obtain the constraints shown in table 2 on reverse transfer.

Appendix D. Triple correlations in homogeneous MHD

Let $A_\alpha(\boldsymbol{x})$, $B_\beta(\boldsymbol{x})$ and $C_\gamma(\boldsymbol{x})$ be individual components of three homogeneous random vector fields. The Fourier transform of the triple correlation of these three

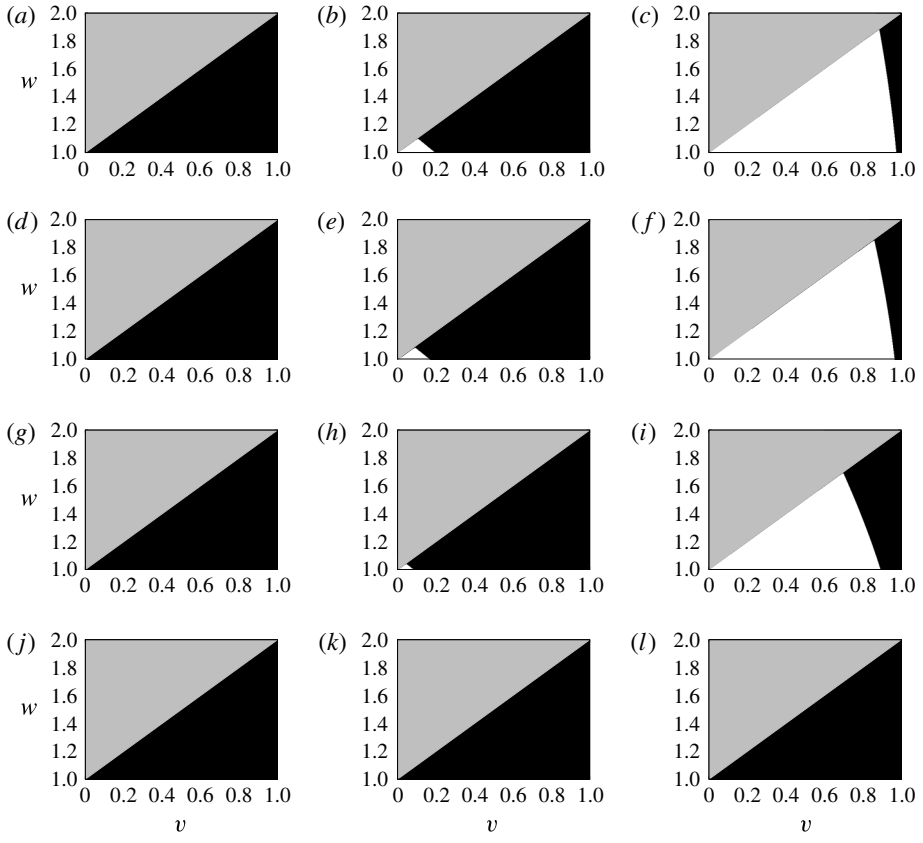

FIGURE 3. Plots of $f(v, w) = x^2 - Q$ for various values of $|U_{s_p}|/|B_{s_p}|$ and cross-helicity for case 3 in appendix C ($s_k = s_p \neq s_q$, $p < k < q$). The upper grey triangle is ruled out by the condition $w < 1 + v$ and unstable values are shown in white. The ratio $|U_{s_p}|/|B_{s_p}|$ increases from left to right, with each column of subfigures taking the values 0.01, 0.1 and 1 respectively, while each row takes the following values of relative cross-helicity: $H_c(p)/(|U_{s_p}||B_{s_p}|) = 0$, 0.5, 0.9 and 1.

fields is

$$\langle \hat{A}_\alpha(\boldsymbol{k})\hat{B}_\beta(\boldsymbol{p})\hat{C}_\gamma(\boldsymbol{q})\rangle = \left(\frac{1}{L}\right)^9 \int\int\int \mathrm{d}^3x\,\mathrm{d}^3x'\,\mathrm{d}^3x''\langle A_\alpha(\boldsymbol{x})B_\beta(\boldsymbol{x}')C_\gamma(\boldsymbol{x}'')\rangle \times \mathrm{e}^{-\mathrm{i}(\boldsymbol{k}\cdot\boldsymbol{x}+\boldsymbol{p}\cdot\boldsymbol{x}'+\boldsymbol{q}\cdot\boldsymbol{x}'')}, \tag{D 1}$$

where the term in the angled brackets on the right-hand side is the real space correlation tensor $C_{\alpha\beta\gamma}$ of the three fields. Since the fields are homogeneous, the real space correlator only depends on the displacements $\boldsymbol{r} = \boldsymbol{x} - \boldsymbol{x}'$ and $\boldsymbol{r}' = \boldsymbol{x} - \boldsymbol{x}''$ and as such is independent of $\boldsymbol{x}$

$$\langle A_\alpha(\boldsymbol{x})B_\beta(\boldsymbol{x}')C_\gamma(\boldsymbol{x}'')\rangle = C_{\alpha\beta\gamma}(\boldsymbol{r}, \boldsymbol{r}'). \tag{D 2}$$

The integration over $\boldsymbol{x}$ then results in a delta function imposing the condition that the triple correlation in Fourier space is non-zero only when the wavevectors form a triad,

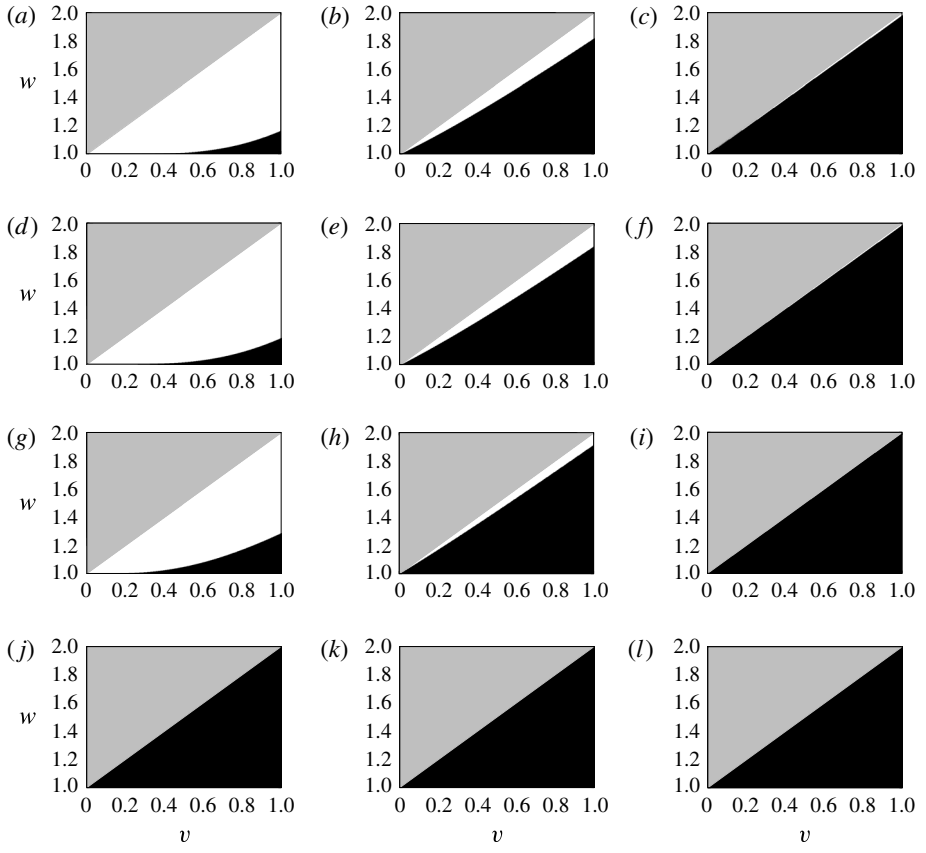

FIGURE 4. Plots of $f(v, w) = x^2 - Q$ for various values of $|U_{s_p}|/|B_{s_p}|$ and cross-helicity for case 4 in appendix C ($s_k = s_p = s_q$, $k < q < p$). The upper grey triangle is ruled out by the condition $w < 1 + v$ and unstable values are shown in white. The ratio $|U_{s_p}|/|B_{s_p}|$ increases from left to right, with each column of subfigures taking the values 1, 10 and 100 respectively, while each row takes the following values of relative cross-helicity: $H_c(p)/(|U_{s_p}||B_{s_p}|) = 0,\ 0.5,\ 0.9$ and 1.

i.e.

$$\langle \hat{A}_\alpha(\boldsymbol{k})\hat{B}_\beta(\boldsymbol{p})\hat{C}_\gamma(\boldsymbol{q})\rangle = \delta(\boldsymbol{k}+\boldsymbol{p}+\boldsymbol{q})\left(\frac{1}{L}\right)^6 \int\int \mathrm{d}^3 r\, \mathrm{d}^3 r'\, C_{\alpha\beta\gamma}(\boldsymbol{r}, \boldsymbol{r}')\mathrm{e}^{-\mathrm{i}(\boldsymbol{p}\cdot\boldsymbol{r}+\boldsymbol{q}\cdot\boldsymbol{r}')}. \quad \text{(D 3)}$$

Since the fields $\boldsymbol{A}$, $\boldsymbol{B}$ and $\boldsymbol{C}$ were arbitrary homogeneous random fields, this result holds for any combination of triple correlations of the magnetic and velocity fields in homogeneous MHD turbulence.

Appendix E. Similarity scaling

For theoretical convenience we assume that both kinetic and magnetic energy spectra have power-law scalings in the inertial range, that is

$$E_{kin}(\alpha k)/E_{kin}(k) = \alpha^{-n}, \quad E_{mag}(\alpha k)/E_{mag}(k) = \alpha^{-m} \quad \text{(E 1}a,b\text{)}$$

where α is a real number and $n > 0$ and $m > 0$ are the spectral indices of the kinetic and magnetic energy spectra, respectively. From

$$E_{kin}(k)\,\mathrm{d}k = \frac{1}{2}\int_{|\boldsymbol{k}|=k} \langle |u_+(\boldsymbol{k})|^2 + |u_-(\boldsymbol{k})|^2\rangle\,\mathrm{d}\boldsymbol{k}, \tag{E 2}$$

$$E_{mag}(k)\,\mathrm{d}k = \frac{1}{2}\int_{|\boldsymbol{k}|=k} \langle |b_+(\boldsymbol{k})|^2 + |b_-(\boldsymbol{k})|^2\rangle\,\mathrm{d}\boldsymbol{k}, \tag{E 3}$$

we then find a scaling of the helical coefficients

$$u_s(\alpha\boldsymbol{k}) = \alpha^{-(5+n)/2}u_s(\boldsymbol{k}), \quad b_s(\alpha\boldsymbol{k}) = \alpha^{(-5+m)/2}b_s(\boldsymbol{k}). \tag{E 4a,b}$$

From (E 1a,b) the scaling of $T^{(i)}_{HD}(k,p,q)$, $T^{(i)}_{LF}(k,p,q)$ and $T^{(i)}_{mag}(k,p,q)$ is then given by

$$\frac{T^{(i)}_{HD}(\alpha k,\alpha p,\alpha q)}{T^{(i)}_{HD}(k,p,q)} = \alpha^{-(1+3n)/2} = \alpha^{-\beta}, \tag{E 5}$$

$$\frac{T^{(i)}_{LF}(\alpha k,\alpha p,\alpha q)}{T^{(i)}_{LF}(k,p,q)} = \alpha^{-(1+n+2m)/2} = \alpha^{-\beta'}, \tag{E 6}$$

$$\frac{T^{(i)}_{mag}(\alpha k,\alpha p,\alpha q)}{T^{(i)}_{mag}(k,p,q)} = \alpha^{-(1+n+2m)/2} = \alpha^{-\beta'}, \tag{E 7}$$

In hydrodynamics $n = 5/3$, while in MHD there are different predictions for the spectral exponent, either $m = 3/2$ (Iroshnikov–Kraichnan) or $m = 5/3$ (Kolmogorov). Note that $n = m = 5/3$ implies $\beta' = \beta = 3$ while $n = 5/3$ and $m = 3/2$ implies $\beta' = 2 + 5/6$. In both cases $\beta - 2 > 0$.

REFERENCES

Alexakis, A., Mininni, P. D. & Pouquet, A. 2005 Shell-to-shell energy transfer in magnetohydrodynamics. I. Steady state turbulence. *Phys. Rev.* E **72**, 046301.

Alexakis, A., Mininni, P. D. & Pouquet, A. 2006 On the inverse cascade of magnetic helicity. *Astrophys. J.* **640**, 335–343.

André, J. C. & Lesieur, M. 1977 Influence of helicity on the evolution of isotropic turbulence at high Reynolds number. *J. Fluid Mech.* **81**, 187–207.

Balsara, D. & Pouquet, A. 1999 The formation of large-scale structures in supersonic magnetohydrodynamic flows. *Phys. Plasmas* **6**, 89–99.

Berera, A. & Linkmann, M. F. 2014 Magnetic helicity and the evolution of decaying magnetohydrodynamic turbulence. *Phys. Rev.* E **90**, 041003(R).

Biferale, L., Musacchio, S. & Toschi, F. 2012 Inverse energy cascade in three-dimensional isotropic turbulence. *Phys. Rev. Lett.* **108**, 164501.

Biferale, L., Musacchio, S. & Toschi, F. 2013 Split energy-helicity cascades in three dimensional homogeneous and isotropic turbulence. *J. Fluid Mech.* **730**, 309–327.

Biferale, L. & Titi, E. S. 2013 On the global regularity of a helical-decimated version of the 3D Navier–Stokes equation. *J. Stat. Phys.* **151**, 1089.

Biskamp, D. 1993 *Nonlinear Magnetohydrodynamics*, 1st edn. Cambridge University Press.

Boffetta, G. & Musacchio, S. 2010 Evidence for the double cascade scenario in two-dimensional turbulence. *Phys. Rev.* E **82**, 016307.

Brandenburg, A. 2001 The inverse cascade and nonlinear alpha-effect in simulations of isotropic helical magnetohydrodynamic turbulence. *Astrophys. J.* **550**, 824–840.

BRANDENBURG, A. 2003 The helicity issue in large scale dynamos. In *Turbulence and Magnetic Fields in Astrophysics* (ed. E. Falgarone & T. Passot), Lecture Notes in Physics, vol. 614, pp. 402–413. Springer.

BRANDENBURG, A., KAHNIASHVILI, T. & TEVZADZE, A. G. 2015 Nonhelical inverse transfer of a decaying turbulent magnetic field. *Phys. Rev. Lett.* **114**, 075001.

BRISSAUD, A., FRISCH, U., LÉORAT, J., LESIEUR, M. & MAZURE, A. 1973 Helicity cascades in fully developed isotropic turbulence. *Phys. Fluids* **16**, 1366.

CARATI, D., DEBLIQUY, O., KNAEPEN, B., TEACA, B. & VERMA, M. 2006 Energy transfers in forced MHD turbulence. *J. Turbul.* **7**, 1–12.

CHEN, Q., CHEN, S. & EYINK, G. L. 2003*a* The joint cascade of energy and helicity in three-dimensional turbulence. *Phys. Fluids* **15**, 361–374.

CHEN, Q., CHEN, S., EYINK, G. L. & HOLM, D. D. 2003*b* Intermittency in the joint cascade of energy and helicity. *Phys. Rev. Lett.* **90**, 214503.

CHILDRESS, S. & GILBERT, A. D. 1995 *Stretch, Twist, Fold: The Fast Dynamo*. Springer.

CHO, J. 2010 Non-locality of hydrodynamic and magnetohydrodynamic turbulence. *Astrophys. J.* **725**, 1786–1791.

CHO, J. 2011 Magnetic helicity conservation and inverse energy cascade in electron magnetohydrodynamic wave packets. *Phys. Rev. Lett.* **106**, 191104.

CHRISTENSSON, M., HINDMARSH, M. & BRANDENBURG, A. 2001 Inverse cascade in decaying 3D magnetohydrodynamic turbulence. *Phys. Rev.* E **64**, 056405.

COBURN, J. T., SMITH, C. W., VASQUEZ, B. J., FORMAN, M. A. & STAWARZ, J. E. 2014 Variable cascade dynamics and intermittency in the solar wind at 1 AU. *Astrophys. J.* **713**, 920–934.

CONSTANTIN, P. & MAJDA, A. 1988 The Beltrami spectrum for incompressible flows. *Commun. Math. Phys.* **115**, 435–456.

DEBLIQUY, O., VERMA, M. K. & CARATI, D. 2005 Energy fluxes and shell-to-shell transfers in three-dimensional decaying magnetohydrodynamic turbulence. *Phys. Plasmas* **12**, 042309.

DUBIEF, Y., TERRAPON, V. E. & SORIA, J. 2013 On the mechanism of elasto-inertial turbulence. *Phys. Fluids* **25**, 110817.

FRISCH, U. 1995 *Turbulence: The Legacy of Kolmogorov*. Cambridge University Press.

FRISCH, U., POUQUET, A., LÉORAT, J. & MAZURE, A. 1975 Possibility of an inverse cascade of magnetic helicity in magnetohydrodynamic turbulence. *J. Fluid Mech.* **68**, 769–778.

KARIMABADI, H., ROYTERSHTEYN, V., WAN, M., MATTHAEUS, W. H., DAUGHTON, W., WU, P., SHAY, M., LORING, B., BOROVSKY, J., LEONARDIS, E., CHAPMAN, S. C. & NAKAMURA, T. K. M. 2013 Coherent structures, intermittent turbulence, and dissipation in high-temperature plasmas. *Phys. Plasmas* **20**, 012303.

KRAICHNAN, R. H. 1967 Inertial ranges in two-dimensional turbulence. *Phys. Fluids* **10** (10), 1417.

KRAUSE, F. & RÄDLER, K. 1980 *Mean-Field Magnetohydrodynamics and Dynamo Theory*. Pergamon Press, Ltd.

LESSINNES, T., PLUNIAN, F. & CARATI, D. 2009 Helical shell models for MHD. *Theor. Comput. Fluid Dyn.* **23**, 439–450.

MCCOMB, W. D. 2014 *Homogeneous, Isotropic Turbulence: Phenomenology, Renormalization and Statistical Closures*. Oxford University Press.

MININNI, P. D. 2011 Scale interactions in magnetohydrodynamic turbulence. *Annu. Rev. Fluid Mech.* **43**, 377–397.

MININNI, P. D., ALEXAKIS, A. & POUQUET, A. 2005 Shell-to-shell energy transfer in magnetohydrodynamics. II. Kinematic dynamo. *Phys. Rev.* E **72**, 046302.

MININNI, P. D., ALEXAKIS, A. & POUQUET, A. G. 2009 Scale interactions and scaling laws in rotating flows at moderate rossby numbers and large Reynolds numbers. *Phys. Fluids* **21**, 015108.

MININNI, P. D. & POUQUET, A. 2013 Inverse cascade behavior in freely decaying two-dimensional fluid turbulence. *Phys. Rev.* E **87**, 033002.

MOFFATT, H. K. 1969 The degree of knottedness of tangled vortex lines. *J. Fluid Mech.* **35**, 117–129.

MOFFATT, H. K. 1978 *Magnetic Field Generation in Electrically Conducting Fluids*. Cambridge University Press.

MÜLLER, W. C., MALAPAKA, S. K. & BUSSE, A. 2012 Inverse cascade of magnetic helicity in magnetohydrodynamic turbulence. *Phys. Rev.* E **85**, 015302.

PARKER, E. N. 1979 *Cosmical Magnetic Fields: their Origin and their Activity*. Clarendon, Oxford University Press.

PELZ, R. B., SHTILMAN, B. & TSINOBER, A. 1986 The helical nature of unforced turbulent flows. *Phys. Fluids* **29**, 3506–3508.

POLIFKE, W. 1991 Statistics of helicity fluctuations in homogeneous turbulence. *Phys. Fluids* A **3**, 115.

POLIFKE, W. & SHTILMAN, L. 1989 The dynamics of helical decaying turbulence. *Phys. Fluids* A **1**, 2025.

POLITANO, H. & POUQUET, A. 1995 Model of intermittency in magnetohydrodynamic turbulence. *Phys. Rev.* E **52**, 636.

POUQUET, A., FRISCH, U. & LÉORAT, J. 1976 Strong MHD helical turbulence and the nonlinear dynamo effect. *J. Fluid Mech.* **77**, 321–354.

POUQUET, A. & PATTERSON, G. S. 1978 Numerical simulation of helical magnetohydrodynamic turbulence. *J. Fluid Mech.* **85**, 305–323.

SAHOO, G., BONACCORSO, F. & BIFERALE, L. 2015 On the role of helicity for large- and small-scales turbulent fluctuations. *Phys. Rev.* E **92**, 051002.

SON, D. T. 1999 Magnetohydrodynamics of the early universe and the evolution of primordial magnetic fields. *Phys. Rev.* D **59**, 063008.

STAWARZ, J. E., SMITH, C. W., VASQUEZ, B. J., FORMAN, M. A. & MACBRIDE, B. T. 2010 The turbulent cascade for high cross-helicity states at 1 AU. *Astrophys. J.* **713**, 920–934.

STEPANOV, R., FRICK, P. & MIZEVA, I. 2015 Joint inverse cascade of magnetic energy and magnetic helicity in MHD turbulence. *Astrophys. J.* **798**, L35.

TITCHMARSH, E. C. 1939 *The Theory of Functions*, 2nd edn. Oxford University Press.

VAINSHTEIN, S. I. & ZELDOVICH, Y. B. 1972 Origin of magnetic fields in astrophysics. *Sov. Phys. Uspekhi* **15**, 159–172.

WALEFFE, F. 1992 The nature of triad interactions in homogeneous turbulence. *Phys. Fluids* A **4**, 350–363.

ZHU, J.-Z., YANG, W. & ZHU, G.-Y. 2014 Purely helical absolute equilibria and chirality of (magneto)fluid turbulence. *J. Fluid Mech.* **739**, 479–501.

ZRAKE, J. 2014 Inverse cascade of nonhelical magnetic turbulence in a relativistic fluid. *Astrophys. J.* **794**, L26.